



Tracing the ecophysiology of ungulates and predator–prey relationships in an early Pleistocene large mammal community

Paul Palmqvist^{a,*}, Juan A. Pérez-Claros^a, Christine M. Janis^b, Darren R. Gröcke^c

^a Departamento de Ecología y Geología, Facultad de Ciencias, Campus Universitario de Teatinos, 29071-Málaga, Spain

^b Department of Ecology and Evolutionary Biology, Brown University, Providence, RI 02912, USA

^c Department of Earth Sciences, Durham University, Science Laboratories, South Road, Durham DH1 3LE, UK

ARTICLE INFO

Article history:
Accepted 25 March 2008

Keywords:
Mammals
Ecomorphology
Biogeochemistry
Pleistocene
Venta Micena
Orce

ABSTRACT

Research into the reconstruction of ancient communities in terms of dietary regimes, habitat preferences and ecological interactions of species has focused predominantly on biogeochemistry or ecomorphology alone and not in combination. The Venta Micena site (Orce, Guadix–Baza basin, SE Spain) has an early Pleistocene vertebrate assemblage with exceptional biomolecular preservation. Collagen was successfully extracted from 77 bone samples of 18 species of large mammals, which allowed analyses of carbon- and nitrogen-isotopes. $\delta^{13}\text{C}$, $\delta^{15}\text{N}$ and $\delta^{18}\text{O}$ ratios combined with ecomorphological indexes provide interesting clues on the autecology and palaeophysiology of extinct species, which help in deciphering aspects of community trophic structure and predator–prey interactions. Specifically, morphometric ratios (e.g., hypsodonty index and relative length of the lower premolar tooth row; [Palmqvist, P., Gröcke, D.R., Arribas, A., Fariña, R. 2003. Paleoeological reconstruction of a lower Pleistocene large mammals community using biogeochemical ($\delta^{13}\text{C}$, $\delta^{15}\text{N}$, $\delta^{18}\text{O}$, Sr:Zn) and ecomorphological approaches. *Paleobiology* 29, 204–228.]) allow classifying the ungulates among grazers (*Equus altidens*, *Bison* sp., *Praeovibos* sp., *Hemitragus albus*, *Hippopotamus antiquus*, and *Mammuthus meridionalis*), mixed-feeders (*Soergelia minor* and *Pseudodama* sp.) and browsers (*Stephanorhinus* sp. and *Praemegaceros* cf. *verticornis*). However, $\delta^{13}\text{C}$ values reveal that these ungulates consumed exclusively C_3 plants and significant differences in isotopic values between perissodactyls (monogastric, hindgut fermenters) and ruminants (foregut fermenters) must reflect physiological differences related to their rates of methane production and digestive efficiency. $\delta^{18}\text{O}$ ratios allow the interpretation of the dietary water source of these species, suggesting that fallow deer *Pseudodama* sp., goat *H. albus* and ovibovine *S. minor* obtained a significant fraction of their metabolic water from the vegetation consumed. Carnivore species have higher $\delta^{15}\text{N}$ values than herbivores, which records the isotopic enrichment expected with an increase in trophic level. However, the unexpectedly high $\delta^{15}\text{N}$ values of hippo *H. antiquus* and muskoxen *Praeovibos* sp. suggest that these ungulates predominantly consumed aquatic plants and lichens, respectively. Inferences on predator–prey relationships within this ancient community, derived from the dual linear mixing model, indicate resource partitioning among sympatric predators, suggesting that sabre-tooth *Megantereon whitei* and jaguar *Panthera* cf. *gombaszoegensis* were ambushers of forest environments while sabre-tooth *Homotherium latidens* and wild dog *Lycaon lycaonoides* were coursing predators in open habitat. The giant, short-faced hyena *Pachycrocuta brevirostris* scavenged the prey of these hypercarnivores.

© 2008 Elsevier B.V. All rights reserved.

1. Introduction: the early Pleistocene locality of Venta Micena

Venta Micena lies near the village of Orce (Granada, SE Spain) in the eastern sector of the Guadix–Baza Basin (37°44′15″N, 2°24′9″W, elevation 974.5 m; Fig. 1). This sedimentary basin was characterized by interior drainage from the end of the Miocene to middle-late Pleistocene times, which facilitated the preservation of Plio-Quaternary large mammal assemblages in swampy and lacustrine sediments.

The site is dated by biostratigraphy to the lower Pleistocene (Arribas and Palmqvist, 1999), with an age estimated in ~1.5 Ma.

The Venta Micena stratigraphic column shows alternate micrite limestone, calcilutitic, lutitic, silty, and marly levels (Fig. 1). The main excavation quarry (VM-2 level, Quarry 3 and drillings 1–4, ~320 m²; Palmqvist and Arribas, 2001) is located within the upper part of the section, in an 80–120 cm thick limestone stratum undisturbed by tectonic activity, composed of homogeneous and porous micrite sediments (98–99% CaCO₃) that can be followed across ~2.5 km in the Orce area (Arribas and Palmqvist, 1998). The lower half of the stratum has carbonate nodules (5–20 cm thick), mud banks and fossil shells of eurythermal freshwater molluscs. During this lacustrine stage, micrite

* Corresponding author. Fax: +34 952137386.
E-mail address: ppb@uma.es (P. Palmqvist).

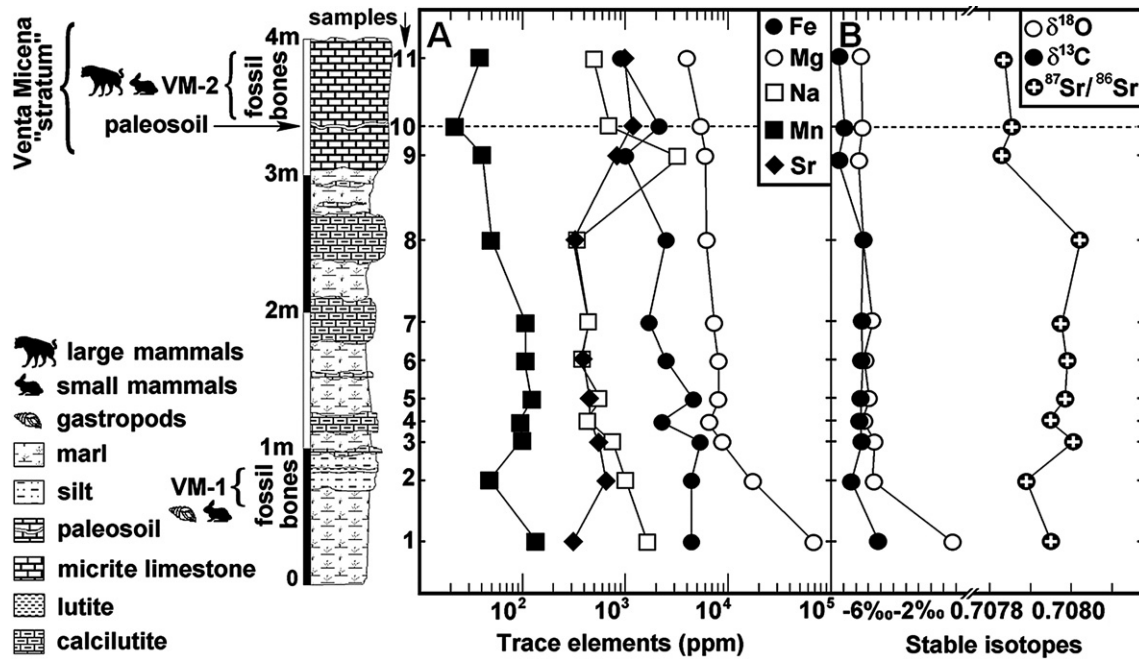


Fig. 1. A: average values of trace-elements (Fe, Mg, Na, Mn, and Sr, in ppm), and B: bulk rock stable-isotope ratios ($\delta^{13}\text{C}$ and $\delta^{18}\text{O}$, in ‰, $^{87}\text{Sr}/^{86}\text{Sr}$) in the samples of sediment collected from the stratigraphic column of the early Pleistocene locality of Venta Micena. C: reconstruction of paleoenvironmental changes in the lake at Venta Micena during early Pleistocene times, inferred from the abundance of trace elements and bulk-rock $\delta^{18}\text{O}$ analyses in samples collected through the Venta Micena stratigraphic section.

was precipitated in a shallow (<10 m), well-oxygenated water sheet not subject to eutrophic conditions, as indicated by the absence of pyrite and carbonate facies rich in organic matter. Above this level there is a 4–15 mm thick calcareous palaeosol, which records a major retreat of the Pleistocene lake and represents a swampy biotope with wide emerged zones (~4 km width) and shallow ponds (<1 m depth, 2–20 m diameter). The upper half of the stratum is composed of micrite sediments showing root marks and mud cracks at the bottom, which record the rise of the lake level, and preserves a high density of fossil bones.

The large mammal assemblage is composed of ~5,800 identifiable skeletal remains from 225 individuals belonging to 21 taxa of large (>5 kg) mammals and ~10,000 unidentifiable bone shafts and cranial fragments. Herbivorous taxa dominate the assemblage in number of identifiable specimens (NISP) and estimates of minimal number of individuals (MNI). The surface of the skeletal remains is not abraded and the longitudinal axes of long bones show no preferred orientation, which indicates that they were not transported by fluvial processes prior to deposition. Furthermore, the ratio of isolated teeth to vertebrae (0.94:1) is close to the value expected in the absence of hydrodynamic sorting (1:1) and the frequencies of bones grouped according to their potential for dispersal by water (i.e., Voorhies's groups) are similar to those in the mammalian skeleton (Arribas and Palmqvist, 1998). Analysis of weathering stages indicates a short time of exposure before burial, less than one year in most cases. Analysis of mortality patterns deduced for ungulate species from juvenile/adult proportions reveals that most skeletal remains were scavenged by the giant, short-faced hyena *Pachycrocuta brevirostris* from carcasses of animals hunted selectively by hypercarnivores (Palmqvist et al., 1996). Taphonomic analysis shows that the hyenas transported ungulate carcasses and body parts to their maternity dens as a function of the mass of the ungulates scavenged. The fracturing of major limb bones in the dens was also highly selective, correlating well with their marrow contents and mineral densities (Palmqvist and Arribas, 2001).

Palaeoecological analyses include inferences on the life style and preferred habitat of extinct taxa (palaeoautecology) and the reconstruction of past ecological associations (palaeosynecology) (Damuth, 1992). Once the preservational completeness of the fossil assemblage

has been evaluated with taphonomic analysis, it is necessary to infer the autecological characteristics of the species prior to synecological analysis at the community level. Autecological properties of extinct taxa may be reconstructed through: 1) ecomorphological inferences on functional adaptations for feeding behaviour and types of locomotion; 2) biogeochemical analyses for reconstructing dietary niches, habitat preferences and palaeotemperatures; and 3) studies of the sedimentary context and taphonomic attributes of the fossils as well as on their distribution across facies (Wing et al., 1992; Palmqvist et al., 2003; Soligo and Andrews, 2005). Once this goal is achieved, species can be distributed among size classes and ecological categories, and the relative frequencies of these categories in the assemblage are compared with those in modern ecosystems (Andrews et al., 1979; Reed, 1998; Mendoza et al., 2005).

Feeding preferences of extinct mammals can be addressed using biogeochemical markers such as stable-isotopes and trace-elements, as well as from the comparative study of their craniodental morphology, because several features of the skull, mandible and dentition are indicative of diet (see reviews in MacFadden, 2000; Williams and Kay, 2001; Mendoza et al., 2002; Palmqvist et al., 2003). In herbivores, the hypsodonty index (HI, unworn molar crown height divided by molar width) discriminates between grazers (>75% grass in diet), which feed upon grasses with high silicophytolith contents and have hypsodont, high-crowned molars, from browsers (<25% grass in diet), which consume succulent leaves and have brachydont, low-crowned teeth. However, although HI is probably the best single variable correlated with diet in living ungulates (and thus of the best use for predicting the diet of extinct ones), in some species molar crown height alone may be insufficient to determine their feeding preferences (Fortelius and Solounias, 2000; Mendoza et al., 2002; Mendoza and Palmqvist, 2008). Muzzle shape also provides information on diet, as it reflects the adaptations related to the "cropping mechanism", including the shape of the premaxilla and the relative proportions of the incisor teeth (Janis and Ehrhardt, 1988; Solounias and Moelleken, 1993; Pérez-Barbería and Gordon, 2001): browsers have narrow muzzles consisting of a rounded incisor arcade with the first incisor generally larger than the third, while grazers have broad muzzles with transversely straight incisor arcades, showing equal or sub-equal sized

Table 1

Height (m), trace-element abundance (ppm) and bulk-rock stable-isotope ratios ($\delta^{13}\text{C}$, $\delta^{18}\text{O}$, in ‰; $^{87}\text{Sr}/^{86}\text{Sr}$) of sedimentary samples (vm-1 to vm-10) collected through the stratigraphic section of Venta Micena

Sample	Height	Fe	Mg	Na	Mn	Sr	Ca	$\delta^{13}\text{C}$	$\delta^{18}\text{O}$	$^{87}\text{Sr}/^{86}\text{Sr}$
vm-11	3.85	897	3975	500	40	979	303,917	-7.36	-5.57	0.707836
vm-10	3.35	2143	5556	682	22	1197	279,964	-6.98	-5.40	0.707857
vm-9	3.15	1007	6068	3245	40	831	297,197	-7.42	-5.75	0.707826
vm-8	2.50	2486	6202	334	50	327	195,090	-5.19	-5.18	0.708020
vm-7	1.95	1695	7396	438	107	435	256,736	-5.60	-4.80	0.707972
vm-6	1.65	2526	8101	389	105	414	236,984	-5.23	-5.18	0.707990
vm-5	1.40	4551	8146	554	120	447	224,936	-5.31	-4.93	0.707989
vm-4	1.15	2256	6465	430	93	449	260,913	-5.61	-5.37	0.707947
vm-3	1.05	5366	8768	754	95	555	202,355	-5.53	-4.31	0.708008
vm-2	0.85	4401	17445	1019	48	647	137,997	-6.34	-4.59	0.707891
vm-1	0.40	4400	68451	1656	136	313	126,781	-4.12	1.79	0.707949

teeth. There are, however, some second-order differences related to the phylogenetic legacy: equids have relatively narrower muzzles than grazing ruminants of similar body size. In addition, different ungulate groups have adopted different solutions when faced with the same ecological specialization: for example, the lower premolars are enlarged in grazing perissodactyls, but grazing ruminants and camelids show the opposite trend. This difference is probably due to differences in the way food is orally processed in foregut and hindgut fermenters (Mendoza et al., 2002).

In carnivores, craniodental features related to diet include the morphology of the upper canine, the size of the trigonid blade and the talonid basin in the lower carnassial, and the shape of the glenoid and angular processes in the mandible, which reflect the moment arms for jaw adductor muscles (Van Valkenburgh, 1988; Biknevicius and Van Valkenburgh, 1996). These variables help in discriminating among hypercarnivores, bone-crackers and omnivores. Relevant features of the postcranial skeleton include the brachial and crural indexes (i.e., radius length divided by humerus length and tibia length divided by femur length, respectively), the ratio of phalanx length to metacarpal length, the biceps brachii leverage index, and cross-sectional geometric properties of major limb bones (Van Valkenburgh, 1985; Anyonge, 1996; Lewis, 1997). These variables estimate different aspects related to habitat preferences and hunting techniques: for example, the brachial and crural indexes are useful for discriminating between predators that ambush their prey in forested environments and those that pursue it in open habitat (Palmqvist et al., 2003).

2. Sedimentary geochemistry and palaeoenvironmental inferences

The trace-element and stable-isotope chemistry of lake waters is a sensitive monitor of climate in arid and semi-arid regions (see review in Hu et al., 1998). Data of trace-element abundance and stable-isotope ratios in the stratigraphic section of Venta Micena (Table 1; Fig. 1A–B) show several key relationships. For example, sodium concentrations decrease systematically from the base of the section, reach their lowest values in the middle of the section, and then suddenly rise to high values below the palaeosoil (Fig. 1A). If sodium concentrations are assumed as representative of lake salinity levels, they show that the middle part of the section witnessed an increase in the water level and/or a reduction of salinity, although the salinity level dramatically increased just prior to palaeosoil development, evidencing the lowering of the water table. Iron and manganese concentrations decrease from level VM-1 to level VM-2, suggesting a shift from a restricted, stratified water column (decreased oxygen levels, stagnation) to a more open, well-oxygenated water column. This evidence supports the increase in lake-level in the middle of the section, as indicated by sodium concentrations, which resulted in increased water supply and, thus, circulation.

Magnesium and strontium concentrations decrease and increase, respectively, through the whole stratigraphic section (Fig. 1A). Magnesium and strontium concentrations are under saturated with

respect to the minerals commonly precipitated within lakes and for this reason both elements have been used for reconstructing changes in water lake salinity levels (Chivas et al., 1985). Magnesium also correlates negatively with water temperature (Chivas et al., 1986). However, on the basis of these bulk-rock analyses, a similar assumption would be difficult here, because magnesium and strontium are negatively correlated in the Venta Micena section.

Oxygen-isotope analyses of the bulk-rock samples show a general decrease to more negative $\delta^{18}\text{O}$ values through the section (Fig. 1B), paralleling the magnesium concentration record. This indicates that magnesium and $\delta^{18}\text{O}$ are negatively correlated with the palaeotemperature of the lake waters and, thus, an overall warming from level VM-1 to the development of the palaeosoil at level VM-2. Sodium and strontium concentrations should be negatively correlated if strontium measures palaeosalinity levels, what is not reflected in the Venta Micena section. However, in a palaeohydrochemical study of a nearby early Pleistocene shallow lacustrine section from Orce, Anadón and Julià (1990) found lower Sr/Ca values in ostracod shells from sands deposited during saline water phases than in those from the overlying carbonate sequences formed under lower salinity conditions; such unexpected values were interpreted as the result of major changes in the chemical composition of the water in shallow swamped areas of a hydrologically complex lake. A subsequent study (Anadón et al., 1994) revealed higher $\delta^{18}\text{O}$ ratios in ostracod shells from intervals with a saline fauna than in those with a freshwater fauna, what is also recorded in the bulk-rock analyses of the Venta Micena section (Fig. 1B). According to Anadón et al. (1994), this would correspond to an alternation of concentration/dilution phases in a shallow lacustrine sequence that correlates with the climatic cycles described in synchronous ocean basin records from the late Matuyama chron. Anadón et al. (1994) also found a covariant trend in $\delta^{13}\text{C}$ and $\delta^{18}\text{O}$ values from ostracod calcite, which indicates that the ostracods lived in a closed lacustrine system. $\delta^{13}\text{C}$ and $\delta^{18}\text{O}$ ratios are also correlated in the Venta Micena section (Fig. 1B).

Bulk-rock $\delta^{13}\text{C}$ ratios are, however, an archive of more difficult interpretation. They show the maximum value in the marly level at the base of the section, fluctuate in the silty, lutitic and calcilitic levels placed in the section from 0.85 m to 2.5 m, and then show a slight decrease in the micrite levels (Fig. 1B). Organic residues in modern soils reflect the $\delta^{13}\text{C}$ of the overlying flora (Koch, 1998). Because its carbon is derived from soil CO_2 , the $\delta^{13}\text{C}$ of soil carbonate is strongly correlated to that of soil organic matter. Atmospheric CO_2 has a higher $\delta^{13}\text{C}$ value (-6.5‰) than both C_3 plants (-26‰) and C_4 plants (-12‰), contributing to soil CO_2 near the surface; however, the CO_2 > 30 cm deep in soils with moderate to high respiration rates is largely supplied by plant decay and root respiration. Both processes generate CO_2 isotopically similar to organic matter. Diffusion of CO_2 from the soil to the atmosphere leads to a $\delta^{13}\text{C}$ enrichment of +4.5‰ for CO_2 at depth in a soil relative to soil organic matter. Finally, temperature-dependent fractionation associated with precipitation of calcite sum to a $\delta^{13}\text{C}$ increase of +10.5‰ (Koch, 1998). As a consequence, modern

Table 2
C:N proportions and isotopic ratios from collagen ($\delta^{13}\text{C}$, $\delta^{15}\text{N}$) and hydroxylapatite ($\delta^{18}\text{O}$) extracted from bone and tooth samples of large mammal species preserved in the early Pleistocene locality of Venta Micena (juv.: juvenile, subad.: subadult; ad.: adult)

Species	Sample code	Fossil specimen (tooth or bone portion)	$\delta^{13}\text{C}_{\text{col}}$	$\delta^{15}\text{N}_{\text{col}}$	$\delta^{18}\text{O}_{\text{hyd}}$	C:N _{col}
<i>Mammuthus meridionalis</i> (juv.)	VM-4439	Proximal metacarpal	-21.4	+4.7	-4.5	3.1
<i>Mammuthus meridionalis</i> (juv.)	VM-0X1	Enamel fragment of deciduous tooth	-	-	-3.9	-
<i>Mammuthus meridionalis</i> (juv./subad.)	VM-3581	Vertebrae fragment (neural arch)	-20.6	+2.9	-2.8	3.3
<i>Mammuthus meridionalis</i> (juv./subad.)	VM-3581b	Vertebrae fragment (neural arch)	-23.4	+4.3	-5.3	3.6
<i>Mammuthus meridionalis</i> (subad./ad.)	VM-2172	Carpal bone	-21.1	+3.2	-5.9	3.4
<i>Mammuthus meridionalis</i> (subad./ad.)	VM-4482	Carpal bone	-	-	-4.7	-
<i>Mammuthus meridionalis</i> (juv.)	VM-4607	Cranial fragment of a newborn individual or fetus	-22.8	+3.5	-4.5	3.5
<i>Mammuthus meridionalis</i> (juv.)	VM-4607b	Cranial fragment of a newborn individual or fetus	-22.9	+3.2	-4.5	3.2
<i>Mammuthus meridionalis</i> (juv.)	VM-84-C3-C8-49	Left maxilla with dP ² and dP ³ partially worn	-	-	-4.5	-
<i>Mammuthus meridionalis</i> (juv.)	VM-4439b	Proximal metacarpal	-23.4	+3.8	-5.3	3.2
<i>Mammuthus meridionalis</i> (juv.)	VM-3674	Vertebrae fragment	-	-	-5.0	-
cf. <i>Mammuthus meridionalis</i> (juv.)	VM-4332	Right humeral diaphysis of a newborn individual	-	-	-1.4	-
cf. <i>Mammuthus meridionalis</i> (juv.)	VM-1919	Left humeral diaphysis of a newborn individual	-22.2	+5.1	-5.6	3.6
Mean for <i>Mammuthus</i> (N=8/13)			-22.23±1.08	+3.84±0.79	-4.45±1.21	3.36±0.19
<i>Hippopotamus antiquus</i> (ad.)	VM-4123	Right fifth metacarpal	-22.3	+7.7	-2.1	3.5
<i>Hippopotamus antiquus</i> (ad.)	VM-0X6	Enamel fragment of permanent tooth	-	-	-5.8	3.4
<i>Hippopotamus antiquus</i> (ad.)	VM-4299	Left proximal humerus	-22.6	+7.4	-3.7	3.4
<i>Hippopotamus antiquus</i> (ad.)	VM-3680	Left femur	-21.2	+7.1	-5.8	3.5
<i>Hippopotamus antiquus</i> (juv.)	VM-3558	Right femur	-	-	-6.2	-
<i>Hippopotamus antiquus</i> (juv.)	VM-3337	Left femur	-23.0	+5.7	-7.3	3.4
<i>Hippopotamus antiquus</i> (juv.)	VM-84-C1-V5-13	Fragment of left mandible with unworn dP ₃ and dP ₄	-22.2	+6.0	-7.6	3.2
Mean for <i>Hippopotamus</i> (N=5/7)			-22.26±0.67	+6.78±0.88	-5.50±1.96	3.40±0.12
<i>Bison</i> sp. (ad.)	VM-3473	Right proximal metacarpal	-22.1	+3.8	-2.2	3.1
<i>Bison</i> sp. (ad.)	VM-3503	Distal metatarsal	-21.5	+3.6	-4.1	3.3
<i>Bison</i> sp. (ad.)	VM-4185	Left proximal metacarpal	-	-	-2.8	-
<i>Bison</i> sp. (ad.)	VM-4444	Left proximal metatarsal	-	-	-3.1	-
<i>Bison</i> sp. (ad.)	VM-0X7	Enamel fragment of permanent tooth	-	-	-5.2	-
<i>Bison</i> sp. (ad.)	VM-3583	Left distal humerus	-	-	-3.7	-
<i>Bison</i> sp. (ad.)	VM-3473b	Right proximal metacarpal	-21.4	+3.5	-3.2	3.3
<i>Bison</i> sp. (ad.)	VM-544	Left distal humerus	-21.8	+4.0	-4.3	3.4
<i>Bison</i> sp. (ad.)	VM-4164	Left distal humerus	-	-	-3.3	-
<i>Bison</i> sp. (juv.)	VM-4378	Right mandible with dP ₂ -dP ₄ and unworn M ₁	-22.7	+4.6	-3.5	3.5
<i>Bison</i> sp. (juv./subad.)	VM-non coded	Right maxilla with unworn P ² -P ⁴ and M ¹	-22.4	+3.1	-4.8	3.6
Mean for <i>Bison</i> (N=6/11)			-21.98±0.51	+3.77±0.51	-3.85±1.08	3.37±0.18
<i>Praeovibos</i> sp. (ad.)	VM-1742	Left metacarpal with fused epiphyses	-22.0	+6.7	-4.7	3.2
<i>Soergelia minor</i> (ad.)	VM-3448	Right distal tibia	-	-	-2.7	-
<i>Soergelia minor</i> (ad.)	VM-3867	Left metatarsal	-23.2	+3.2	-2.1	3.4
<i>Soergelia minor</i> (ad.)	VM-3867b	Left metatarsal	-23.5	+3.4	-2.3	3.5
<i>Soergelia minor</i> (ad.)	VM-0X10	Enamel fragment of permanent tooth	-	-	-2.6	-
<i>Soergelia minor</i> (ad.)	VM-3982	Left proximal metatarsal	-23.0	+3.8	-2.7	3.3
<i>Soergelia minor</i> (subad.)	VM-4597	Maxilla with unworn P ² -P ⁴ and M ¹ -M ³ erupting	-23.9	+2.2	-	3.6
<i>Soergelia minor</i> (ad.)	VM-4336	Right horn base	-23.4	+4.3	-2.3	3.2
Mean for <i>Soergelia</i> (N=5/5)			-23.40±0.34	+3.38±0.78	-3.16±1.88	3.40±0.16
<i>Hemitragus albus</i> (ad.)	VM-3802	Left distal metatarsal	-20.9	+4.0	-3.4	3.3
<i>Hemitragus albus</i> (ad.)	VM-3922	Right distal metacarpal	-20.1	+3.9	-1.5	3.4
<i>Hemitragus albus</i> (ad.)	VM-0X11	Enamel fragment of permanent tooth	-	-	-3.3	-
<i>Hemitragus albus</i> (ad.)	VM-3157	Distal metatarsal	-	-	-2.1	-
<i>Hemitragus albus</i> (ad.)	VM-3449	Left distal humerus	-20.4	+3.7	-2.9	3.5
<i>Hemitragus albus</i> (ad.)	VM-4541a	Distal right humerus with fused epiphysis	-21.6	+3.4	-3.6	3.6
Mean for <i>Hemitragus</i> (N=4/6)			-20.75±0.66	+3.75±0.26	-2.80±0.83	3.45±0.13
<i>Pseudodama</i> sp. (ad.)	VM-3055	Right proximal metatarsal	-	-	-3.2	-
<i>Pseudodama</i> sp. (ad.)	VM-3482	Left proximal metacarpal	-23.6	+2.5	-2.6	3.5
<i>Pseudodama</i> sp. (ad.)	VM-4330	Left proximal metacarpal	-	-	-2.4	-
<i>Pseudodama</i> sp. (ad.)	VM-0X9	Enamel fragment of permanent tooth	-	-	-2.6	-
<i>Pseudodama</i> sp. (ad.)	VM-4410	Fragment of left hemimandible with M ₁ -M ₃	-	-	-2.9	-
<i>Pseudodama</i> sp. (ad.)	VM-3047	Right distal metacarpal	-23.8	+2.9	-3.0	3.3
<i>Pseudodama</i> sp. (ad.)	VM-3060	Right proximal metacarpal	-23.2	+2.6	-2.5	3.4
<i>Pseudodama</i> sp. (subad.)	VM-4409	Left mandible with dP ₄ heavily worn and M ₁	-22.8	+1.8	-2.8	3.2
<i>Pseudodama</i> sp. (subad.)	VM-4037	Right mandible with dP ₃ -dP ₄ and M ₁ slightly worn	-22.2	+2.2	-1.3	3.0
Mean for <i>Pseudodama</i> (N=5/9)			-23.12±0.64	+2.40±0.42	-2.59±0.55	3.28±0.19
<i>Praemegaceros verticornis</i> (ad.)	VM-3297	Fragment of right metacarpal diaphysis	-25.9	+1.6	-3.3	3.2
<i>Praemegaceros verticornis</i> (ad.)	VM-4155	Left proximal radius	-	-	-2.8	-
<i>Praemegaceros verticornis</i> (ad.)	VM-3111	Distal metacarpal	-	-	-4.0	-
<i>Praemegaceros verticornis</i> (ad.)	VM-3556	Right distal humerus	-25.6	+1.3	-4.2	3.6
<i>Praemegaceros verticornis</i> (ad.)	VM-0X8	Enamel fragment of permanent tooth	-	-	-4.6	-
<i>Praemegaceros verticornis</i> (ad.)	VM-4181	Left distal humerus	-25.4	+1.8	-3.7	3.4
<i>Praemegaceros verticornis</i> (ad.)	VM-3111b	Distal metacarpal	-	-	-3.9	-
<i>Praemegaceros verticornis</i> (ad.)	VM-3224	Left distal metatarsal	-25.8	+1.4	-3.1	3.5
<i>Praemegaceros verticornis</i> (ad.)	VM-3780	Left distal humerus	-	-	-4.0	-
<i>Praemegaceros verticornis</i> (juv.)	VM-84C3-E10-63	Left mandible with dP ₂ -dP ₄	-25.9	+2.3	-3.5	3.4
<i>Praemegaceros verticornis</i> (juv.)	VM-82-9	Left maxilla with dP ² , dP ³ and dP ⁴	-24.4	+1.7	-	3.3
<i>Praemegaceros verticornis</i> (juv.)	VM-4039	Right mandible with dP ₄ and M ₁ erupting	-25.2	+2.0	-3.7	3.6
<i>Praemegaceros verticornis</i> (juv.)	VM-4394	Fragment of right maxilla, with dP ² , dP ³ , dP ⁴ and M ¹	-	-	-2.0	-
Mean for <i>Praemegaceros</i> (N=7/12)			-25.46±0.53	+1.73±0.35	-3.80±1.07	3.43±0.15
<i>Stephanorhinus etruscus</i> (ad.)	VM-4487	Left proximal ulna	-26.5	+3.9	-3.7	3.5

Table 2 (continued)

Species	Sample code	Fossil specimen (tooth or bone portion)	$\delta^{13}\text{C}_{\text{col}}$	$\delta^{15}\text{N}_{\text{col}}$	$\delta^{18}\text{O}_{\text{hyd}}$	C:N _{col}
<i>Stephanorhinus etruscus</i> (ad.)	VM-4510	Right humeral diaphysis	-26.6	+3.7	-3.7	3.3
<i>Stephanorhinus etruscus</i> (ad.)	VM-OX4	Tooth fragment	-	-	-3.7	-
<i>Stephanorhinus etruscus</i> (ad.)	VM-OX5	Enamel fragment of permanent tooth	-	-	-5.1	-
<i>Stephanorhinus etruscus</i> (ad.)	VM-3616	Right distal femur	-26.2	+3.5	-4.2	3.3
<i>Stephanorhinus etruscus</i> (ad.)	VM-3578	Left scapula	-	-	-4.6	-
<i>Stephanorhinus etruscus</i> (ad.)	VM-3578b	Left scapula	-	-	-4.8	-
<i>Stephanorhinus etruscus</i> (ad.)	VM-3578c	Left scapula	-25.8	+3.0	-5.2	3.2
<i>Stephanorhinus etruscus</i> (ad.)	VM-3744	Right femoral diaphysis	-24.7	-	-4.3	3.1
<i>Stephanorhinus etruscus</i> (juv./subad.)	VM-1908	Right distal radius with the epiphysis unfused	-25.2	+3.6	-4.8	3.6
<i>Stephanorhinus etruscus</i> (juv.)	VM-non coded	Fragment of left maxilla, with dP ² and dP ³	-	-	-3.9	-
Mean for <i>Stephanorhinus</i> (N=6/11)			-25.83±0.76	+3.22±0.85	-4.36±0.57	3.33±0.19
<i>Equus altidens</i> (ad.)	VM-3028	Right metatarsal lacking the distal epiphysis	-26.1	+2.0	-2.5	3.2
<i>Equus altidens</i> (ad.)	VM-3119	Right scapula	-26.7	+3.5	-2.8	3.6
<i>Equus altidens</i> (ad.)	VM-3162	Right distal tibia	-26.0	+3.0	-3.0	3.5
<i>Equus altidens</i> (ad.)	VM-3258	Right distal tibia	-	-	-2.9	-
<i>Equus altidens</i> (ad.)	VM-3430	Left distal metatarsal	-	-	-2.3	-
<i>Equus altidens</i> (ad.)	VM-3529	Left proximal scapula	-26.0	+3.3	-3.3	3.4
<i>Equus altidens</i> (ad.)	VM-4189	Fragment of metatarsal diaphysis	-25.5	+3.5	-2.3	3.5
<i>Equus altidens</i> (ad.)	VM-4421	Left proximal radius	-25.0	+2.1	-3.8	3.4
<i>Equus altidens</i> (ad.)	VM-OX2	Enamel fragment of permanent tooth	-	-	-3.4	-
<i>Equus altidens</i> (ad.)	VM-OX3	Enamel fragment of permanent tooth	-	-	-5.2	-
<i>Equus altidens</i> (ad.)	VM-3089	Left distal metacarpal	-	-	-3.5	-
<i>Equus altidens</i> (ad.)	VM-4421b	Left proximal radius	-25.8	+2.8	-3.9	3.4
<i>Equus altidens</i> (ad.)	VM-3279	Left tibia diaphysis	-26.6	+3.1	-4.3	3.5
<i>Equus altidens</i> (ad.)	VM-3428	Distal diaphysis of metatarsal	-	-	-2.8	-
<i>Equus altidens</i> (juv./subad.)	VM-4403	Maxilla with worn dP ¹ -dP ⁴ , M ¹ -M ³ erupting	-25.8	+3.5	-2.5	3.6
<i>Equus altidens</i> (juv.)	VM-602	Metacarpal with the proximal epiphysis unfused	-26.3	+2.0	-3.7	3.1
<i>Equus altidens</i> (juv.)	VM-2073	Right metacarpal, two thirds of proximal diaphysis	-	-	-4.3	-
<i>Equus altidens</i> (juv.)	VM-3388	Right mandible fragment with unworn dP ₂ -dP ₄	-25.1	+2.6	-5.2	3.5
Mean for <i>Equus</i> (N=11/18)			-25.90±0.55	+2.85±0.60	-3.43±0.90	3.43±0.16
<i>Hystrix major</i> (ad.)	VM-93-3B-96	Fragment of incisor tooth	-	-	-3.5	-
<i>Pachyrocute brevisrostris</i> (ad.)	VM-2226	Ulna	-22.5	+6.1	-4.0	3.4
<i>Pachyrocute brevisrostris</i> (ad.)	VM-2004	Third proximal diaphysis of radius	-	-	-3.9	-
<i>Pachyrocute brevisrostris</i> (ad.)	VM-2276	Right mandible with M ₁	-23.0	+4.7	-5.2	3.5
<i>Pachyrocute brevisrostris</i> (juv.)	VM-460	Skull fragment with left dP ³ and dP ⁴	-	-	-3.5	-
<i>Pachyrocute brevisrostris</i> (juv.)	VM-84-C3-H5-6	Left mandible with dP ₂ and dP ₃	-21.5	+5.8	-2.3	3.6
<i>Pachyrocute brevisrostris</i> (juv.)	VM-non coded	Fragment of maxilla of a juv. individual	-21.5	+6.7	-3.7	3.0
Mean for <i>Pachyrocute</i> (N=4/6)			-22.12±0.75	+5.82±0.84	-3.77±0.93	3.37±0.26
<i>Homotherium latidens</i> (ad.)	VM-4340	Right distal tibia of an ad. individual	-21.7	+6.8	-3.7	3.4
<i>Homotherium latidens</i> (ad.)	VM-4340b	Right distal tibia of an ad. individual	-22.7	+6.5	-5.0	3.6
<i>Homotherium latidens</i> (ad.)	VM-4516	Left humerus of an ad. individual	-23.9	+5.6	-4.7	3.4
Mean for <i>Homotherium</i> (N=3/3)			-22.77±1.10	+6.30±0.62	-4.47±0.68	3.47±0.12
<i>Megantereon whitei</i> (ad.)	VM-3301	Left distal humerus of an ad. individual	-25.2	+5.8	-4.2	3.5
<i>Megantereon whitei</i> (ad.)	VM-4612	Right distal humerus of an ad. individual	-24.4	+5.1	-5.0	3.4
Mean for <i>Megantereon</i> (N=2/2)			-24.80±0.57	+5.45±0.49	-4.60±0.57	3.45±0.07
<i>Panthera cf. gombaszoegensis</i> (ad.)	VM-84-C3-F8-42	Fragment of right mandible	-23.3	+5.0	-4.3	3.0
<i>Ursus etruscus</i> (ad.)	VM-1172	Right distal radius	-	-	-3.3	-
<i>Ursus etruscus</i> (ad.)	VM-2972	Right tibia of an ad. individual	-23.8	+6.7	-0.4	3.3
<i>Ursus etruscus</i> (ad.)	VM-1903	Left radius of an ad. individual	-21.9	+7.4	-1.9	3.1
<i>Ursus etruscus</i> (ad.)	VM-non coded	Skull	-23.6	+6.0	-2.0	3.3
Mean for <i>Ursus</i> (N=3/4)			-23.10±1.04	+6.70±0.70	-1.90±1.19	3.23±0.12
<i>Lycaon lycaonoides</i> (ad.)	VM-2261	Right maxilla with P ₄ -M ₁	-22.7	+6.5	-4.8	3.5
<i>Lycaon lycaonoides</i> (ad.)	VM-2263	Skull (splashed and deformed) of an ad. individual	-23.8	+5.6	-5.9	3.5
<i>Lycaon lycaonoides</i> (ad.)	VM-2259	Fragment of right maxilla of an ad. individual, with M ¹	-22.9	+5.2	-3.7	3.4
Mean for <i>Lycaon</i> (N=3/3)			-23.13±0.59	+5.77±0.67	-4.80±1.10	3.47±0.06
<i>Canis mosbachensis</i> (ad.)	VM-2254	Left mandible with M ₂ and roots of P ₃ -P ₄ -M ₁	-23.5	+5.3	-4.8	3.6
<i>Canis mosbachensis</i> (ad.)	VM-2254b	Left mandible with M ₂ and roots of P ₃ -P ₄ -M ₁	-21.8	+4.1	-3.7	3.5
<i>Canis mosbachensis</i> (subad.)	VM-4440	Right mandible, M ₁ with non developed roots	-22.2	+4.7	-4.6	3.3
Mean for <i>Canis</i> (N=3/3)			-22.50±0.89	+4.70±0.60	-4.37±0.59	3.47±0.15

carbonates forming below 30 cm depth have $\delta^{13}\text{C}$ values ~15‰ higher on average than those of organic matter: -11‰ for soils with C₃ overlying flora and +3‰ for soils in which organic matter is supplied by C₄ plants (Koch, 1998). The range of $\delta^{13}\text{C}$ ratios measured in the Venta Micena stratigraphic section (-4.1‰ to -7.4‰) lies between both values, suggesting a mixed vegetation of C₃ and C₄ plants. However, $\delta^{13}\text{C}$ values for bone collagen of grazing ungulates (see below) show the absence of C₄ grasses in their diet. This indicates that other factors apart from changes in primary productivity and respiration in the water column may also have been involved in determining bulk-rock $\delta^{13}\text{C}$ ratios; for example, under higher pressures of atmospheric CO₂, more of the CO₂ at depth in soils would be derived from the atmosphere, increasing the difference in $\delta^{13}\text{C}$ values between soil carbonate and organic matter (Koch, 1998).

In a recent study of a 356-m-thick composite section of the Guadix-Baza basin that ranges from the late Pliocene to the middle Pleistocene, Ortiz et al. (2006) interpreted the $\delta^{13}\text{C}$ and $\delta^{18}\text{O}$ profiles as reflecting changes in temperature, the evaporation/infill ratio in the water bodies and the amount of rain. Specifically, they concluded that high $\delta^{13}\text{C}$ and $\delta^{18}\text{O}$ values were associated with warm and dry regimes, whereas low $\delta^{13}\text{C}$ and $\delta^{18}\text{O}$ values correlated with cold and humid episodes, which caused more vegetation biomass and, therefore, an increase in the input of isotopically light carbon.

Strontium isotopes (⁸⁷Sr/⁸⁶Sr) can be used for deriving the palaeosalinity record of ancient environments if independent constraints on the system's hydrologic parameters (i.e., evaporation, precipitation, fluvial and ocean exchange fluxes) are available (e.g., salinity estimates provided by lithology and faunal assemblages;

Flecker et al., 2002). $^{87}\text{Sr}/^{86}\text{Sr}$ ratios of river waters are similar to those of terrestrial plants and there are no significant differences in ^{87}Sr contents between grasses and trees (Hoppe et al., 1999). In herbivores, the $\delta^{87}\text{Sr}$ value of bioapatite equals the average ratio of the vegetation ingested, which in turn monitors the soluble strontium in soils, derived from weathering and precipitation. Environmental $^{87}\text{Sr}/^{86}\text{Sr}$ ratios vary with differences in atmospheric input as well as with differences in bedrock age and composition (Price et al., 1985; Miller et al., 1993). Due to this reason, variations in $\delta^{87}\text{Sr}$ have been used for reconstructing migratory behaviour in a variety of vertebrates, including proboscideans (Koch et al., 1995; Hoppe et al., 1999; Hoppe, 2004). Concerning the stratigraphy of Venta Micena (Fig. 1B), bulk-rock $^{87}\text{Sr}/^{86}\text{Sr}$ ratios are relatively uniform in the lower part of the section, with the only exception of a decrease in level VM-1. This reflects deposition under conditions of hydrological stability. The upper carbonate samples, however, show a significant decrease in $^{87}\text{Sr}/^{86}\text{Sr}$ proportions, which reflects an increase in river or ground-water input that translated in the rising of the lake's table in the lacustrine levels.

3. Stable-isotope analyses of the Venta Micena fauna

Stable isotopes have proved useful in determining the dietary niches of extinct mammals, providing detailed ecological and environmental reconstructions. Published carbon-, nitrogen- and oxygen-isotopes of collagen and hydroxylapatite from 18 species of large mammals identified in the Venta Micena assemblage (Gröcke et al., 2002; Palmqvist et al., 2003; $N=65$) and results obtained from additional samples ($N=50$; Table 2) of juvenile individuals and species not sampled in the previous study (e.g., *Praeovibos* sp., *Hystrix major*, *Panthera cf. gombaszoegensis*, and *Ursus etruscus*) are analyzed here to determine their dietary niches and predator–prey relationships. Collagen was successfully extracted from 77 bone samples, which allowed analyses of carbon- and nitrogen-isotopes. Oxygen-isotopes were retrieved from 115 bone and tooth hydroxylapatite samples. The precision for stable-isotope analysis was 0.1‰ for both carbon and oxygen, and 0.2‰ for nitrogen. Carbonate carbon and oxygen isotopic analyses were performed using a Fison Optima isotope-ratio mass-spectrometer, with a common acid bath system in the Stable-Isotope Biogeochemistry Laboratory at McMaster University. Samples were reacted with 100% phosphoric acid at 90 °C. Collagen carbon and nitrogen isotopic analyses were performed at the Stable-Isotope Biogeochemistry Laboratory at McMaster University using a Thermo-Finnigan DeltaPlus XP coupled with a Costech elemental analyzer.

Stable isotopes are useful palaeobiological tracers because, as a result of mass differences, different isotopes of an element have different thermodynamic and kinetic properties, leading to measurable isotopic partitioning during physical and chemical processes, which labels the substances with distinct isotopic ratios (Gröcke, 1997a; Koch, 1998). Isotopic ratios are reported as parts per thousand (‰) of deviation from a standard, using the δ notation, where:

$$\delta X = \left[\left(\frac{R_{\text{sample}}}{R_{\text{standard}}} \right) - 1 \right] \cdot 1000,$$

where, $X = ^{13}\text{C}$, ^{15}N or ^{18}O , and $R = ^{13}\text{C}/^{12}\text{C}$, $^{15}\text{N}/^{14}\text{N}$ or $^{18}\text{O}/^{16}\text{O}$. R_{sample} and R_{standard} are the high-mass to low-mass isotope ratios of the sample and the standard, respectively. Common standards for $\delta^{13}\text{C}$, $\delta^{15}\text{N}$ and $\delta^{18}\text{O}$ are Peedee belemnite (PDB), atmospheric N_2 and standard mean ocean water (SMOW), respectively.

The measurement of carbon- and nitrogen-isotope ratios in an animal's bone collagen provides an indication of aspects of its overall diet for the last few years of life (DeNiro and Epstein, 1978). Apart from a report on bone collagen preserved in Late Cretaceous dinosaurs (Ostrom et al., 1993), original carbon- and nitrogen-isotope compositions have been retrieved from organic residues in fossils as old as 200 ka (Jones et al., 2001), though adequate preservation in such

ancient specimens is rare (Bocherens et al., 1996a; Gröcke, 1997a). Thus, the extraction of collagen from 77 out of 105 fossil bone samples of Venta Micena, a locality with an age of ~1.5 Ma, constitutes an example of unusual biomolecular preservation. It is worth mentioning that other fossil proteins (e.g., albumin and immunoglobulin) have also been detected in fossil samples from this site using immunological techniques (Torres et al., 2002).

Several methods are available to identify alteration of collagen, including analysis of C:N ratios (between 2.9 and 3.6) and amino acid composition (Gröcke, 1997a; Richards et al., 2000; Drucker et al., 2003). These criteria allow for the identification and exclusion of collagen that is heavily degraded and/or contaminated. This is not the case at Venta Micena, because C:N ratios of the collagen material extracted averaged 3.18 (Table 2) and the amino acid composition from four specimens is similar to that of bone collagen in modern mammals, indicating good preservation (Palmqvist et al., 2003; Fig. 6).

3.1. Carbon-isotopes and palaeodiet

Terrestrial plants can be divided into two main groups on the basis of their photosynthetic pathway (Edwards and Walker, 1983): 1) C_3 plants, which follow the Calvin–Benson cycle (atmospheric CO_2 is fixed through the reductive pentose phosphate pathway); and 2) C_4 plants, which use the Hatch–Slack cycle (C_4 -dicarboxylic acid pathway). C_3 plants are all trees and bushes, temperate shrubs and grasses adapted to cool/moist climate and/or high altitude, whereas C_4 plants include tropical, arid-adapted grasses. All plants take up $^{12}\text{CO}_2$ in preference to $^{13}\text{CO}_2$, but are important differences in their isotopic composition related to their carboxylating enzymes (Smith and Epstein, 1971; Gröcke, 1997b; Koch, 1998). C_3 plants use the ribulose carboxylase and have an average $\delta^{13}\text{C}$ value of $-26.0 \pm 2.3\%$ (range: from -35% in closed canopy to -20% in open areas exposed to water stress). C_4 plants use the phosphoenolpyruvate carboxylase, which discriminates less effectively against $^{13}\text{CO}_2$, showing a mean $\delta^{13}\text{C}$ value of $-12.0 \pm 1.1\%$ (range: -19% to -8%).

When plants are consumed by herbivores, the plant carbon is incorporated into their skeletal tissues with some additional fractionation. The difference between the $\delta^{13}\text{C}$ value of the animal's diet and that subsequently incorporated into bone collagen ($\delta^{13}\text{C}_c$) translates in an average increase per trophic level of $+1.0\%$ (range: 0% to $+4.5\%$) and a similar enrichment is recorded in carnivores (see review in Bocherens and Drucker, 2003). The isotope enrichment factor for biogenic apatite is higher, $+14.1\%$ on average for ungulates (Cerling et al., 2003).

3.2. Nitrogen-isotopes and trophic level

The nitrogen-isotope composition of collagen in mammals records their position in the trophic web, since each trophic level above herbivore is indicated by a mean increase in $\delta^{15}\text{N}$ of $\sim 3.4\%$ (range: 1.7% to 6.9% ; Robinson, 2001; Bocherens and Drucker, 2003; Vanderklift and Ponsard, 2003). Soil synthesis of nitrogen, the diet of the animal (i.e., if it consumes N_2 -fixing or non- N_2 -fixing plants) and nitrogen metabolism are the primary factors that affect the $\delta^{15}\text{N}$ value expressed in herbivore collagen (Sealy et al., 1987; Virginia et al., 1989; Bocherens et al., 1996b; Gröcke et al., 1997; Koch, 1998; Robinson, 2001). Herbivores from closed environment show lower $\delta^{15}\text{N}$ values than those from open grassland because of soil acidity in dense forest. Plants that fix nitrogen have $\delta^{15}\text{N}$ values that cluster close to the atmospheric N_2 value of 0% , whereas those that do not fix nitrogen and use other sources (e.g., soil NH_4^+ and NO_3^-) show a wider range of values. Therefore, animals consuming N_2 -fixing plants will generally exhibit $\delta^{15}\text{N}$ values between 0% and 4% , while herbivores feeding on non- N_2 -fixing plants will show $\delta^{15}\text{N}$ values comprised between 2% and 8% . Plants near marine or salt-affected areas show enrichment in $\delta^{15}\text{N}$ values and deep-rooted plants are enriched over those with shallow roots.

The effects of nitrogen metabolism in mammals are very important. Higher $\delta^{15}\text{N}$ values are observed in mammals inhabiting arid regions, due to ecophysiological differences in nitrogen metabolism associated with adaptations for drought tolerance: under conditions of increased aridity, mammals concentrate urine and excrete concentrated urea, subsequently causing elevated $\delta^{15}\text{N}$ values (Gröcke, 1997a; Koch, 1998; Schwarcz et al., 1999). In general, higher $\delta^{15}\text{N}$ values are found in perissodactyls (monogastric, hindgut-fermenting herbivores) than in foregut ruminants (Gröcke and Bocherens, 1996), but the cause behind these elevated values is not clearly understood. Ruminants have a distinct process of nitrogen cycling, where some waste urea is dumped into the rumen, and they are thus less water dependent than monogastric herbivores. Elevated $\delta^{15}\text{N}$ levels may also be indicative of young suckling animals, due to the ingestion of nutrient-enriched milk (Gröcke, 1997a; Jenkins et al., 2001).

3.3. Oxygen-isotopes and water requirements

Oxygen-isotope values in enamel and bone apatite reflect prevailing climatic conditions (e.g., palaeotemperature; Koch et al., 1989; Ayliffe et al., 1992), but they also allow the interpretation of the dietary water source of a local fauna (Sponheimer and Lee-Thorp, 2001; Harris and Cerling, 2002). The oxygen-isotope composition of apatite is a function of three main oxygen sources: atmospheric O_2 , liquid water and oxygen bound in food (Bryant and Froelich, 1995; Bryant et al., 1996; Kohn, 1996; Kohn et al., 1996). Unlike atmospheric O_2 , the $\delta^{18}\text{O}$ composition of food and water are highly variable, and thus likely to explain any differences found in the $\delta^{18}\text{O}$ ratios of sympatric taxa. The $\delta^{18}\text{O}$ in plants is more positive than in their source water, which is ultimately derived from local rain. In most cases, liquid water in plant roots and stems is isotopically similar to drinking water available for herbivores, but leaf water is relatively enriched in H_2^{18}O due to preferential evapotranspiration of the lighter H_2^{16}O molecule. A study of the oxygen isotope composition of modern South African ungulates (Sponheimer and Lee-Thorp, 2001) revealed that mixed-feeding

impalas (*Aepyceros melampus*), grazing tsessebes (*Damaliscus lunatus*) and blue wildebeests (*Connochaetes taurinus*) obtain relatively more of their water from green vegetation and are significantly enriched in ^{18}O compared to other herbivores such as warthog (*Phacochoerus aethiopicus*), waterbuck (*Kobus ellipsiprymnus*) and giraffe (*Giraffa camelopardalis*), which derive more of their total water intake from drinking. Similar differences were detected by Harris and Cerling (2002) between grazing and browsing East African ungulates. Thus, among extinct ungulates a more positive result would indicate that the species obtained most of its water requirements from the plants eaten rather than from drinking. Animal tissues consist mainly of proteins whereas plant tissues consist mainly of carbohydrates. Given that proteins are depleted in ^{18}O compared to carbohydrates, carnivores show lower $\delta^{18}\text{O}$ values than herbivores (Sponheimer and Lee-Thorp, 2001).

4. Trophic level and palaeodietary inferences

Fig. 2 shows a plot of $\delta^{13}\text{C}$ and $\delta^{15}\text{N}$ values measured in large mammals from Venta Micena. The range of $\delta^{13}\text{C}$ values for ungulates (-27‰ to -20‰) agrees with that of modern herbivores eating C_3 plants, which confirms that C_4 grasses were absent from southern Spain during early Pleistocene times (Palmqvist et al., 2003). There are, however, important variations of carbon-isotope ratios among ungulates (Fig. 3), with perissodactyls showing the lowest $\delta^{13}\text{C}$ values (range: -26.7‰ to -24.2‰) and bovids the highest ones (range: -23.9‰ to -20.1‰). This difference is statistically significant ($t=19.25$, $p<0.0001$) and does not seem to indicate a different feeding behaviour for both groups, given their hypsodonty values (HI). In fact, the two perissodactyl species have similar $\delta^{13}\text{C}$ values, but the highly hypsodont cheek teeth (HI=6.1) of horse *Equus altidens* identify it as a grazer (HI=3.9–8.7 for grazing perissodactyls; Mendoza et al., 2002), whereas the brachydont teeth (HI=1.8) of rhino *Stephanorhinus* sp. indicate that it was a mixed feeder or browser (HI=0.8–2.2 for mixed-feeding and browsing perissodactyls; Mendoza et al., 2002). Both

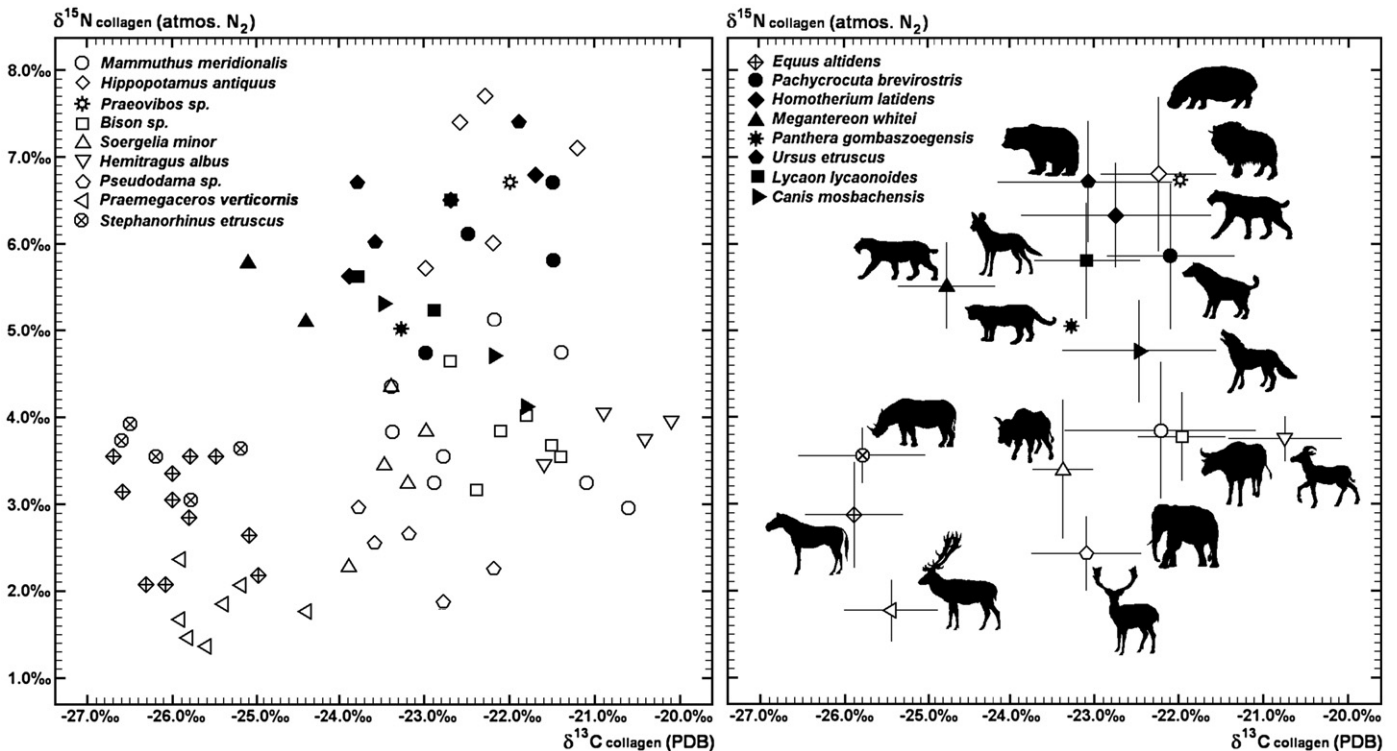


Fig. 2. Plot of $\delta^{13}\text{C}$ and $\delta^{15}\text{N}$ values of collagen material extracted from bone samples of large mammal species preserved in the lower Pleistocene site of Venta Micena (data from Table 2). The lines represent one standard deviation around the mean for those species in which at least two measurements of stable-isotopes were available.

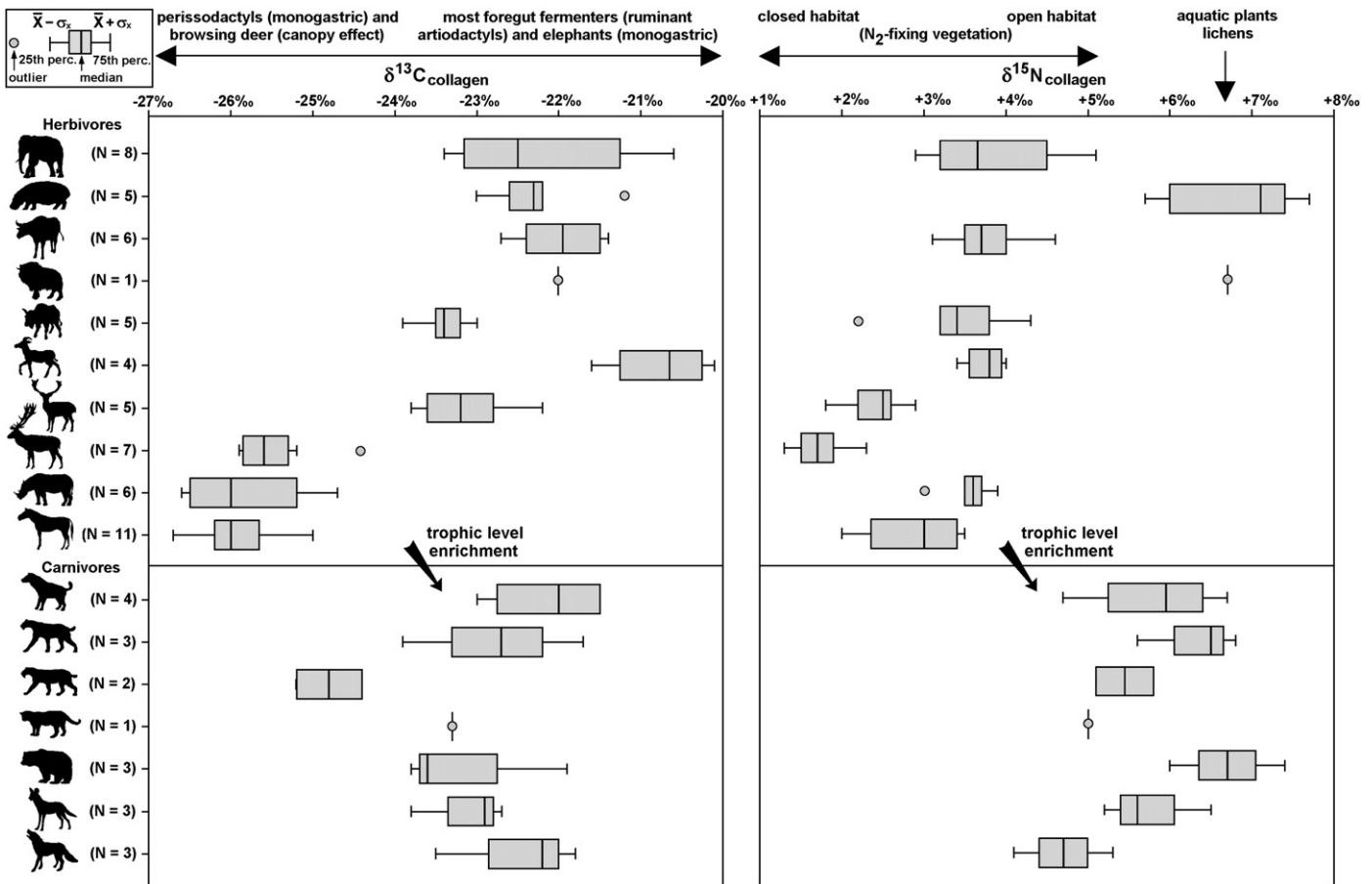


Fig. 3. Box diagrams of $\delta^{13}\text{C}$ and $\delta^{15}\text{N}$ values of collagen material extracted from bone samples of large mammal species preserved in Venta Micena (data from Table 2).

species presumably inhabited open, relatively unforested environments, given their comparatively high $\delta^{15}\text{N}$ values (Fig. 3). Among the bovids, the bovine *Bison* sp. (HI=3.9) and the caprine *Hemitragus albus* (HI=4.4) have moderately hypsodont teeth, indicative of a diet composed mainly of grass (HI=3.8–6.1 for modern grazing bovids; Mendoza et al., 2002). In contrast, the ovibovine *Soergelia minor* has mesodont teeth (HI=2.9), suggestive of a mixed diet (HI=2.5–5.3 for mixed-feeding bovids from open habitat; Mendoza et al., 2002). The relatively high $\delta^{15}\text{N}$ values of all these extinct bovids suggest that they dwelled in unforested environments. Cervids *Praemegaceros* cf. *verticornis* and *Pseudodama* sp. also show lower $\delta^{13}\text{C}$ mean ratios than bovids (-25.9‰ to -22.2‰) ($t=11.71$, $p<0.0001$, two-tailed test). Both species have low-crowned teeth (HI=1.6 and 1.7, respectively), which suggests that they were mixed feeders or browsers in closed habitat, as most cervids (HI=1.1–2.8 in modern deer; Mendoza et al., 2002). In fact, *P. verticornis* shows the lowest $\delta^{15}\text{N}$ contents among ungulates and lower $\delta^{13}\text{C}$ values than other ruminants (Fig. 3), which suggests a browsing diet in closed canopy.

The similarity in $^{13}\text{C}/^{12}\text{C}$ ratios shown by the two perissodactyls is unlikely to indicate similarity in diets, and shared dietary differences to the ruminants, especially as there were no C_4 grasses in this locality. Rather, it reflects a lower isotope enrichment factor for the heavy-carbon isotope in these monogastric herbivores than in ruminants, related to physiological differences between both groups in their digestive systems (hindgut and foregut, respectively). Of interest for this study, Cerling and Harris (1999) found that Burchell's zebras (*Equus burchelli*), whose diet is composed of nearly 100% grass (McNaughton and Georgiadis 1986), are consistently 1–2‰ depleted in $\delta^{13}\text{C}$ values for tooth enamel compared to sympatric ruminant hypergrazers such as alcelaphine bovids; this depletion implies a lower isotope enrichment factor for zebras, resulting from their lower

digestive efficiency. A similar difference was detected by Lee-Thorp and Van der Merwe (1987) between bone bioapatite samples from zebra and wildebeest (*Connochaetes taurinus*). Recent studies of bone collagen isotopes of European fauna over the last glacial cycle and the Holocene also showed consistently 1–2‰ depleted $\delta^{13}\text{C}$ values in horse compared to ruminants (Bocherens and Drucker, 2003; Richards and Hedges, 2003). However, it is worth noting that the difference in $\delta^{13}\text{C}$ ratios between ruminants and perissodactyls in Venta Micena is greater than the differences reported at other sites, which suggests that some dietary differences must be also involved.

The two megaherbivores, elephant *Mammuthus meridionalis* and hippo *Hippopotamus antiquus*, show high $\delta^{13}\text{C}$ values, similar to those of bovids (Fig. 3). The proboscidean seems to have been a mixed feeder like modern African elephants (*Loxodonta africana*), although grass probably was a more significant component of its diet according to carbon-isotopes of tooth enamel in fossil *Mammuthus* from Africa and North America (Koch et al., 1998; Cerling et al., 1999). In the case of *H. antiquus*, the modern hippo, *Hippopotamus amphibius*, is a reputedly grazer that has brachydont teeth, as in the specimens of Venta Micena. The reason for this apparent anomalous condition of low hypsodonty is most likely related to the fact that hippos have low metabolic rates, consuming less food per day than would be expected for animals of their size (Novak, 1999; Schwarm et al., 2006), which translates in a lower amount of wear on the teeth (Mendoza et al., 2002). In addition, a recent study of the isotopic composition of enamel in several African populations of *H. amphibius* has shown that modern hippos have a more varied diet than usually thought, including significant amounts of C_3 plants in closed to moderately open environments (Boisserie et al., 2005).

The higher $\delta^{13}\text{C}$ enrichment of the Venta Micena ruminants, in comparison with the perissodactyls, is probably related to the higher

rates of methane production in the forestomach of ruminants than in the hindgut of monogastric herbivores, which derive a lower fraction of maintenance energy from methanogenic activity of bacteria (Crutzen et al., 1986; Metges et al., 1990; Vermorel et al., 1997; Schulze et al., 1998; Hedges, 2003). However, it seems anomalous that the elephant, a hindgut fermenter, should have an enrichment value that resembles that of the ruminants. However, elephants are not closely related to perissodactyls (Springer et al., 1997) and phylogenetic differences may be at work here. In addition, elephants have a shorter and wider small intestine in comparison to other hindgut fermenters, which is related to the need for animals of such large size to have a very rapid passage rate of the ingesta (Clauss et al., 2003).

The ruminant type of forestomach fermentation provides a clear advantage under conditions of limiting quantities of food: ruminants are very efficient at extracting maximum amounts out of the cellulose and cell contents of food of moderate fibre content, and if feeding on food of relatively good quality they can subsist on a lesser amount of food per day (~70%) than a hindgut fermenter of similar size, which relies on a rapid passage time and the processing of large quantities of food (Janis, 1976; Janis et al., 1984; Duncan et al., 1990). If food is not a limiting factor, however, hindgut fermentation works well with plants of low nutritive value, such as herbage with high fibre contents. This is because a large volume of food can be processed rapidly and the monogastric herbivore can obtain a large quantity of energy from the cell contents in a short time. Among present-day ungulates, the mid range of body sizes (10–1000 kg) is dominated by ruminants. The exceptions are equids, which can feed on low quality grasses too fibrous for a ruminant to subsist on, and tapirs, which have remained as a relict group of tropical forest browsers. There are physiological reasons behind the absence of ruminants at very small body sizes: given that the basal metabolic rate scales allometrically to the 0.75 power of body mass (and a similar exponent applies to food intake rate in herbivores), small animals have relatively greater energetic demands than larger ones (Kleiber, 1975; McNab, 1986; Shipley et al., 1994). Ruminants less than 10 kg (tragulids and duikers) eat primarily non-fibrous food items, such as young leaves, buds, seeds and fruit, and the small herbivores that can subsist on more fibrous diets are all hindgut fermenters such as hyraxes and lagomorphs. Physiological scaling effects also operate at the largest body sizes: as the retention time of food in the digestive tract scales to the 0.27 power of body mass (Illius and Gordon, 1992), there is no advantage to foregut fermentation above a certain body mass (600 kg for browse, 1200 kg for grass forage) in terms of digestive efficiency, because the retention times and percentages of fibre digestibility are similar for both foregut and hindgut fermenters (Demment and Van Soest, 1985; Prins and Kreulen, 1991; Justice and Smith, 1992; Van Soest, 1994). In addition, while specific metabolic rate decreases with increasing mass, gut capacity remains a constant fraction of body size (Bell, 1971; Jarman, 1974; Geist, 1974; Parra, 1978; Justice and Smith, 1992). This implies that larger ungulates are able to support their lower specific metabolic requirements by ingesting forage of lower quality (Van Soest, 1996). Ruminants are at a disadvantage at very large body sizes, as they are unable to accelerate the passage rate of their ingesta, and may suffer from other physiological problems such as a decreased capacity for water retention (Clauss et al., 2003). The observation on the upper size limit for ruminants, based on the range of modern forms, is supported by the fossil record on extinct ruminants and tylopods, which did not, with the possible exception of the sivatheriine giraffids and some Pliocene North American camels, surpass extant species in maximum body size.

The digestive physiology of elephants, however, deviates from the common scheme postulated for herbivores of increasing body mass (Clauss et al., 2003; Loehlein et al., 2003): elephants do not have long ingesta passage rates and achieve only comparatively low digestibility coefficients. As discussed above, the main nutritional advantage of large body size is that larger animals have lower relative energy

requirements and that, due to their increased gastrointestinal tract capacity, they achieve longer ingesta passage rates, which allows them to use forage of lower quality. However, the fermentation of plant material cannot be optimized endlessly, because there is a time when plant fibre is totally fermented and energy losses due to methanogenic bacteria become punitive (Clauss et al., 2003). Therefore, very large herbivores need to evolve adaptations for a comparative acceleration of ingesta passage. Among the extant ungulates, elephants, with their shortened gastrointestinal tract and reduced caecum, are indicators of a trend that allowed even larger hindgut fermenting mammals to exist (Clauss et al., 2003). Foregut fermenting ungulates did not evolve species in which the intake-limiting effect of the foregut could be reduced (e.g., by special bypass structures), and hence their digestive model imposed an intrinsic body size limit for ruminants. This limit will be lower the more the diet enhances the ingesta retention and hence the intake-limiting effect: due to the mechanical characteristics of grass, grazing ruminants cannot become as large as the largest browsing ruminant, the giraffe. In contrast, the design of the gastrointestinal tract of hindgut fermenters allows adaptations for relative passage acceleration, which explains why the largest extinct mammal (*Paraceratherium*, with a body mass of 10,000–15,000 kg; Fortelius and Kappelman, 1993) was a hindgut fermenter (Clauss et al., 2003).

Fig. 3 shows $\delta^{15}\text{N}$ values for the large mammals from Venta Micena. Carnivores *Homotherium latidens*, *Megantereon whitei*, *Panthera cf. gombaszoegensis*, *Pachycrocuta brevirostris*, *Lycaon lycaonoides*, and *Canis mosbachensis* show higher values than ungulates except in the case of *H. antiquus* and the sample analyzed of the single specimen of muskoxen, *Praeovibos* sp., preserved in the assemblage. The isotopic fractionation between carnivores and herbivores is in accordance with the enrichment value expected from increasing one trophic level, indicating that the collagen extracted from the fossils did not undergo diagenetic alteration.

With the only exceptions of hippo and muskoxen, all ungulate species record isotopic values that agree well with a diet of N_2 -fixing plants (Fig. 3). The high $\delta^{15}\text{N}$ values obtained for *H. antiquus*, which are even more elevated than those of the Venta Micena carnivores, suggest that this extinct hippo fed predominantly on aquatic plants, instead of consuming terrestrial grasses as do living hippos (Boissarie et al., 2005). Sealy et al. (1987) found $\delta^{15}\text{N}$ values in *H. amphibius* similar to those of other sympatric grazing artiodactyls from southern Africa that feed on terrestrial vegetation, and smaller than those in carnivores. The unexpected diet of *H. antiquus* probably relates to the huge size of this extinct hippo: preliminary estimates based on the diaphyseal diameter of major limb bones provide a figure of ~3200 kg of average body mass for *H. antiquus* (1500 kg for *H. amphibius*; Novak, 1999). In addition, *H. antiquus* had shorter metapodials than modern hippos. Given the fact that *H. amphibius* is not well designed for dwelling on land, the enormous size and short limbs of *H. antiquus* must have posed even more severe limitations for terrestrial locomotion.

Modern muskoxen (*Ovibos moschatus*) are sexually dimorphic ruminants that live in a highly seasonal environment, consuming willow, forbs and sedge-dominated vegetation types (Klein and Bay, 1994). However, during winter muskoxen subsist primarily on lichens and some senescent browse. Lichens, although potentially high in digestible energy, contain less protein than required for metabolic maintenance. Thus, the elevated $\delta^{15}\text{N}$ value of the single specimen of *Praeovibos* sp. (Fig. 3) could indicate increased recycling of nitrogen from body protein during winter due to a poor quality diet (Barboza and Reynolds, 2004; Parker et al., 2005).

Perissodactyls and bovids show more positive $\delta^{15}\text{N}$ ratios than cervids ($t=7.36$, $p<0.05$) (Fig. 3). This indicates that the cervids would preferably feed in closed habitats, where their low $\delta^{15}\text{N}$ values would result from soil acidity (Rodière et al., 1996; Gröcke, 1997a). Among the perissodactyls, the comparatively high $\delta^{15}\text{N}$ values of the browsing rhino, *Stephanorhinus* sp., suggest that this species lived in open habitat, in a similar fashion to the modern black rhino (*Diceros*

bicornis). $\delta^{15}\text{N}$ values for elephant, *M. meridionalis*, are similar to those expected in a large monogastric herbivore (Gröcke and Bocherens, 1996). $\delta^{15}\text{N}$ values for the horse, *E. altidens*, are also congruent with those of hindgut fermenters of medium size living in an open environment.

Carbon and nitrogen isotopic compositions of collagen provide a proxy to reconstruct ancient trophic webs and especially to decipher the relationships between predators and their potential prey (see review in Bocherens and Drucker, 2003). The wide range of $\delta^{13}\text{C}$ and $\delta^{15}\text{N}$ values in the Venta Micena carnivores reflects resource partitioning among sympatric predators (Figs. 2, 3). For example, sabre-tooth cats *H. latidens* and *M. whitei* have quite distinct isotopic signatures, the former showing the highest $\delta^{13}\text{C}$ values among carnivores and the latter the lowest ones (Fig. 3). This suggests that both predators specialized on different types of ungulate prey, which is confirmed by differences in their postcranial anatomy (Anyonge, 1996; Arribas and Palmqvist, 1999; Palmqvist and Arribas, 2001; Palmqvist et al., 2003). The dirk-tooth *M. whitei* had a robust body, a low brachial index (~80%) and short metapodials, features that describe it as an ambush predator of forested habitat. In such an environment, browsing ungulates with depleted $\delta^{13}\text{C}$ and $\delta^{15}\text{N}$ values would have been the preferred prey. The European jaguar *P. gombaszoegensis* was also an ambusher with a postcranial anatomy similar to that of the extant jaguar (*Panthera onca*). The scimitar-tooth *H. latidens* had comparatively long and slender limbs, and a body size similar to that of a modern lion (*Panthera leo*). The forelimb was more elongated than the hind limb, indicating that the animal probably had

a sloping back. This suggests adaptations to carry away large prey. The claws of *Homotherium* were small, with the exception of a well-developed dewclaw in the first digit of the forefoot. The elongated forelimb (brachial index of ~100%) and small claws suggest increased cursoriality in an open habitat and less prey grappling capability than other sabre-tooth cats (Palmqvist et al., 2003). In such habitat, the prey would be large grazing ruminants and juveniles of megaherbivores, as discussed in depth below.

Canids *L. lycaonoides* and *C. mosbachensis* show intermediate $\delta^{13}\text{C}$ values, while the hyena *P. brevirostris*, the bone-collecting agent at this locality, has the highest $\delta^{13}\text{C}$ values among carnivores. Results obtained in a comparative ecomorphological study of the craniodental anatomy of modern and Pleistocene canids (Palmqvist et al., 1999, 2002) indicate that the larger canid, *L. lycaonoides*, was a hypercarnivore (>70% vertebrate flesh in diet). The postcranial anatomy of this species is similar to that of African hunting dogs (*Lycaon pictus*), the only living canids with a tetradactyl forelimb, which indicates a coursing behaviour. The medium-sized canid, *C. mosbachensis*, has a craniodental anatomy similar to those of modern coyote (*Canis latrans*), with a talonid basin well-developed in the lower carnassial. This suggests an omnivorous diet. The short-faced hyena, *P. brevirostris*, had a body and skull 20% larger than in modern spotted hyenas (*Crocuta crocuta*) and was well-adapted for destroying carcasses and consuming bones (Arribas and Palmqvist, 1998; Palmqvist and Arribas, 2001). This hyaenid differed from other species in the shortening of the distal limb segments, which suggests less coursing abilities, although such shortening would provide greater power and

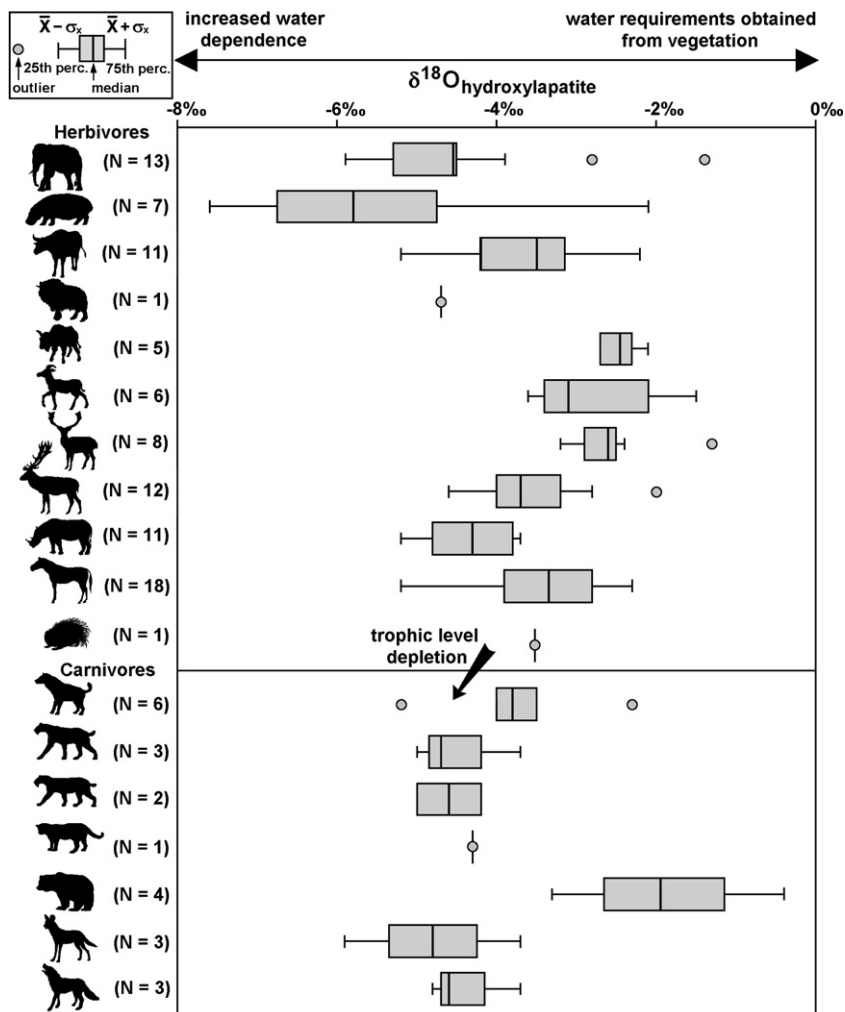


Fig. 4. Box diagrams of $\delta^{18}\text{O}$ values of hydroxylapatite from bone samples and tooth enamel of large mammal species preserved in Venta Micena (data from Table 2).

more stability for dismembering and carrying large pieces of ungulate carcasses (Turner and Antón, 1996).

The high $\delta^{18}\text{O}$ values of cervid *Pseudodama* sp., bovids *H. albus* and *S. minor*, and bear *U. etruscus* (Fig. 4) suggest that these species obtained most of their water requirements from the vegetation rather than from drinking. In contrast, *M. meridionalis*, *H. antiquus*, *Stephanorhinus* sp., *P. verticornis*, and *Praeovibos* sp. exhibit the lowest $\delta^{18}\text{O}$ ratios, which indicate greater water dependence for these species. *Bison* sp. and *E. altidens* show intermediate $\delta^{18}\text{O}$ values but closer to those of megaherbivores and large deer, which suggest moderate water dependence for both grazing species. These results agree with expectations from their living closest relatives (see review in Palmqvist et al., 2003). For example, goats are well-adapted for arid conditions, obtaining most of their water requirements from the vegetation; such physiological specialization seems to have been developed by the caprine *H. albus* and the ovibovine *S. minor*. Modern fallow deer (*Dama dama*) tolerates more arid conditions than red deer (*Cervus elaphus*), showing a lower water intake rate per kg of body mass, and this was clearly the case for *Pseudodama* sp. The largest monogastric mammals from Africa, black rhino, hippo and elephant, show a greater water dependence than grazing ruminants (Bocherens et al., 1996a), which agrees with the low ^{18}O contents of *Stephanorhinus*, *Hippopotamus* and *Mammuthus*, respectively. In fact, Harris and Cerling (2002) found that tooth enamel samples from hippos and elephants from Queen Elizabeth Park, Uganda, were consistently depleted in ^{18}O compared with those from C_4 -grazing ungulates that obtain most of their water from the plants. All carnivore species in Venta Micena show depleted $\delta^{18}\text{O}$ values in comparison with the herbivores, as would be predicted from the higher protein content of their diet (Sponheimer and Lee-Thorp, 2001).

5. Predator–prey relationships

The differences in $\delta^{13}\text{C}$ and $\delta^{15}\text{N}$ values among carnivores (Figs. 2, 3) suggest specific predator–prey relationships in this early Pleistocene community (Palmqvist et al., 1996). For example, *H. latidens* shows the highest $\delta^{13}\text{C}$ and $\delta^{15}\text{N}$ values among hypercarnivores, which would indicate that this was the top predator of the palaeocommunity (i.e., the only one able to hunt on very large prey such as juveniles of megafauna and adult ungulates of medium-to-large size). In contrast, *M. whitei* and *P. gombaszoegensis* show the lowest $\delta^{13}\text{C}$ and $\delta^{15}\text{N}$ ratios, which may

provide evidence that browsing ungulates from forest represented an important fraction of their diet.

Previous studies indicate that primary and secondary productivities of the large mammal fauna from Venta Micena assemblage are balanced, which suggests that all large carnivore species living in the original community were preserved in the bone assemblage collected by the hyenas (Palmqvist et al., 2003). Thus, it seems quite reasonable to assume that the potential prey species for each predator were also preserved in the taphocoenosis. The issue here is to assign the preferred ungulate preys to each predator and to quantify their relative contributions to the predator's diet.

Given that the only sources of carbon and nitrogen for a carnivore come from its diet, the composition of its tissues will be a function of what the animal ate. Using the isotopic enrichment from prey to predator and the principle of mass balance, the dual linear mixing model (Phillips, 2001) allows estimating quantitatively the proportional contribution of several ungulate prey species to the diet of a carnivore. For two isotopes and three prey sources, their relative abundances in the diet of a predator consuming them may be estimated from the following equations:

$$\delta^{13}\text{C}_{\text{predator}} = f_A \delta^{13}\text{C}'_{\text{prey A}} + f_B \delta^{13}\text{C}'_{\text{prey B}} + f_C \delta^{13}\text{C}'_{\text{prey C}},$$

$$\delta^{15}\text{N}_{\text{predator}} = f_A \delta^{15}\text{N}'_{\text{prey A}} + f_B \delta^{15}\text{N}'_{\text{prey B}} + f_C \delta^{15}\text{N}'_{\text{prey C}},$$

$$1 = f_A + f_B + f_C,$$

where $\delta^{13}\text{C}'_{\text{prey}}$ and $\delta^{15}\text{N}'_{\text{prey}}$ are the carbon- and nitrogen-isotope ratios of prey after correction for trophic fractionation, and f represents the relative contributions of preys A, B and C to the diet of predator, respectively. This model has been satisfactorily applied to studies of the diet of living carnivores (Phillips, 2001; Phillips and Koch, 2002; Phillips and Gregg, 2003) as well as to derive inferences on the diet of extinct species, including Neanderthals and anatomically modern humans (Drucker and Bocherens, 2004; Bocherens et al., 2005; Phillips et al., 2005). If an apparently unreasonable solution is obtained for the contribution of a given prey species (i.e., $f < 0$ or > 1), this can mean either that an important food source was not included in the analysis or that trophic correction factors were not estimated appropriately (Phillips, 2001). However, the model will yield correct results if some of the sources are not in the predator's diet and even can be used for

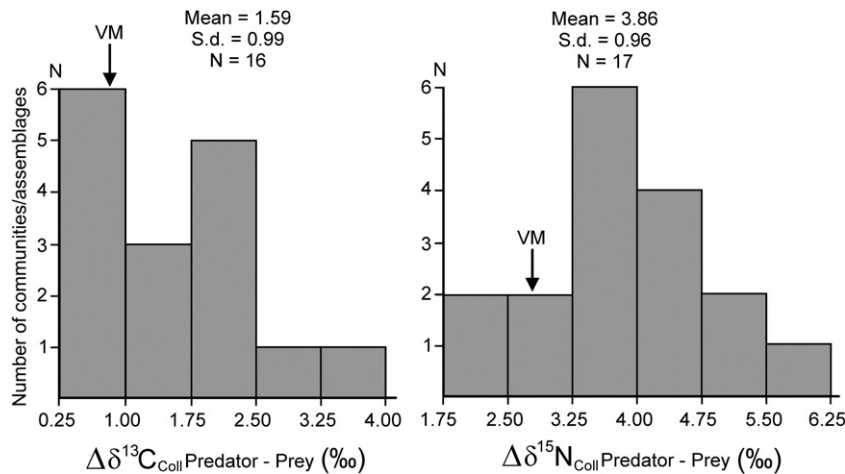


Fig. 5. Histograms showing the distribution of mean values of isotopic enrichment of carbon- and nitrogen-isotopes ($\Delta\delta^{13}\text{C}$ and $\Delta\delta^{15}\text{N}$, respectively) in bone collagen between mammalian carnivores and their potential prey for several living communities and fossil assemblages. Arrows indicate the values for Venta Micena (VM), obtained averaging the species means according to NISP values (*H. antiquus* and *Praeovibos* sp. excluded). Fossil assemblages (late Pleistocene to Holocene): Bocherens et al., 1995 (Kent's Cave, England); Fizet et al., 1995 (Marillac, France); Bocherens et al., 1996a,b (Yakutia, Russia); Gröcke 1997a (Henschke Cave, Australia); Bocherens et al., 1999 (Scladina Cave, Level 4, Belgium); Bocherens et al., 2001 (Scladina Cave, Levels 1A-1B, Belgium); McNulty et al., 2002 (Natural Trap Cave, USA); Bocherens and Drucker, 2003 (Saint Germain — la Rivière, France; Les Jamblands, France); Coltrain et al., 2004 (Rancho La Brea, USA); Drucker and Bocherens, 2004 (Saint Césaire–Camiac–La Berbie, France). Recent communities: Ambrose and DeNiro, 1986 (East Africa); Sealy et al., 1987 (Kasungu National Park, Malawi); Van der Merwe, 1989 (South Africa); Schwarcz, 1991 (Ontario, Canada); Sillen and Lee-Thorp, 1994 (Southwestern Cape, South Africa); Bocherens et al., 1996b (Yakutia, Russia); Szepanski et al., 1999 (Alaska, USA); Bocherens and Drucker, 2003 (Bielowiecza forest, Poland).

investigating the dietary composition of a mixture of more than 'n±1' sources for 'n' isotopes (Phillips and Gregg, 2003; Bocherens et al., 2005).

This methodological approach was applied to the four hypercarnivore species identified at Venta Micena, *H. latidens*, *M. whitei*, *P. gombaszoegensis*, and *L. lycaonoides*. The giant hyena, *P. breviostris*, was excluded from the analysis because taphonomic studies unequivocally indicate that it scavenged the prey of hypercarnivores (Palmqvist et al., 1996; Arribas and Palmqvist, 1998; Palmqvist and Arribas, 2001). The Etruscan bear, *U. etruscus*, was not considered because its teeth are similar to those of modern brown bears (*Ursus arctos*), which is evidence of an omnivorous diet. The craniodental anatomy of the medium-sized canid, *C. mosbachensis*, indicates a more omnivorous behaviour than that of the hunting dog *L. lycaonoides* (Palmqvist et al., 1999, 2002) and was also excluded from subsequent analyses. The comparatively low $\delta^{15}\text{N}$ values of this coyote-like species suggest that invertebrates and fruit were also an important fraction of its diet. However, in the case of the bear, its very high $\delta^{15}\text{N}$ values are intriguing. Perhaps this species consumed regularly fish, in contrast with the other carnivores, or the high $\delta^{15}\text{N}$ values may have resulted from the physiology of dormancy: Fernández-Mosquera et al. (2001) have reported higher $\delta^{15}\text{N}$ values in cave bears (*Ursus spelaeus*) that lived during colder periods, which suggest a reuse of urea in synthesizing amino acids with prolonged duration of dormancy.

Among ungulates, *H. antiquus* was discarded as a potential prey given its enormous size and amphibious behaviour, which makes it difficult to conceive of a predator specializing on it; the scarce remains of this species in the assemblage would be the result of the scavenging activity of hyenas on carcasses of adult animals dead by other causes than predation and juveniles hunted occasionally by sabre-tooth cats (Fig. 7 B). Elephant *M. meridionalis*, however, was analyzed because isotopic data were available for young individuals, the only age stage that would be susceptible to predation according to data on lion predation on modern elephants (see review in Palmqvist et al., 1996). Finally, *Praeovibos* sp. was discarded because this species, poorly represented in the assemblage, presumably lived in mountainous areas, as modern muskoxen.

The first step is to quantify the trophic fractionation ($\Delta\delta^{13}\text{C}$, $\Delta\delta^{15}\text{N}$) between diet and animal tissues, which is not an easy task given that enrichment values depend on the type of food sources and animal tissues analyzed. Trophic fractionation in mink and bear range from -2.2 to 4.9‰ for $\delta^{13}\text{C}$, and from 2.3 to 4.1‰ for $\delta^{15}\text{N}$, respectively (Phillips and Koch, 2002). In a review of studies developed under experimental conditions on isotopic enrichment between diet and collagen, Bocherens and Drucker (2003) found that the enrichment factor ranges from 3.7‰ to 6.0‰ for carbon and from 1.7‰ to 6.9‰ for nitrogen, respectively. These data agree with the commonly quoted ranges for enrichment values of bone collagen of 0 to 2‰ for carbon and 3 to 5‰ for nitrogen. Fig. 5 shows the distribution of differences in $\delta^{13}\text{C}$ and $\delta^{15}\text{N}$ mean values for bone collagen between carnivores and their potential ungulate prey in a set ($N=18$) of modern ecosystems and fossil assemblages compiled from the literature. Dentine collagen was not considered here because it tends to show higher $\delta^{15}\text{N}$ values than bone collagen in some species, probably due to a suckling isotopic signal retained in dentine and eliminated in bone (Bocherens et al., 2001). Although the range of $\Delta\delta^{13}\text{C}$ and $\Delta\delta^{15}\text{N}$ values in these communities is very wide (Fig. 5), the mean fractionations (1.6‰ and 3.8‰, respectively) are close to those reported previously (Phillips and Koch, 2002; Bocherens and Drucker, 2003).

In the case of Venta Micena, the $\Delta\delta^{13}\text{C}$ and $\Delta\delta^{15}\text{N}$ values between herbivores and carnivores, weighted according to NISP values, are 0.8‰ and 2.8‰, respectively. Given that both values are close to the modal classes in the reference dataset (Fig. 5), they were used for correcting the $\delta^{13}\text{C}$ and $\delta^{15}\text{N}$ values of ungulate prey prior to applying the dual linear mixing model to hypercarnivores. It could be argued, however, that it is circular to apply fractionations calculated from the fossil animals whose diets are being reconstructed. However, this is

the most reasonable solution, because in this way the centroids for herbivores and carnivores will match in the plot of $\delta^{13}\text{C}$ and $\delta^{15}\text{N}$ values corrected for trophic fractionation, which guarantees that each predator will be enclosed in a triangle defined by its three main ungulate prey species (Fig. 6). The relative contributions of each ungulate prey to the diet of each hypercarnivore were calculated using the software IsoSource v.1.3.1 (http://www.epa.gov/wed/pages/models/stableisotopes/isosource/IsoSourceV1_3_1.zip).

Obviously, there are many possible solutions for the diet of each predator, but the reasonable ones (i.e., those that do not provide negative estimates for one or more prey species) involve only three possible ungulate prey according to the spatial distribution of predators in the $\delta^{13}\text{C}$ - $\delta^{15}\text{N}$ diagram (see Phillips and Gregg, 2003; Fig. 6). It is worth noting, however, that the software IsoSource allows estimating the dietary contributions of more than three preys. In doing so, the program calculates the mean proportion for each ungulate in the diet of a given predator using the average of the estimates obtained in all the combinations of three potential preys. However, this procedure provides non-unique solutions, which results in increased uncertainty on the source contributions (see discussions in Phillips and Gregg, 2001, 2003; Phillips et al., 2005). In addition, if all ungulate species preserved in the assemblage are considered as a potential prey of each carnivore, this would lead to unrealistic solutions (e.g., to consider that the wild dog *L. lycaonoides* hunted

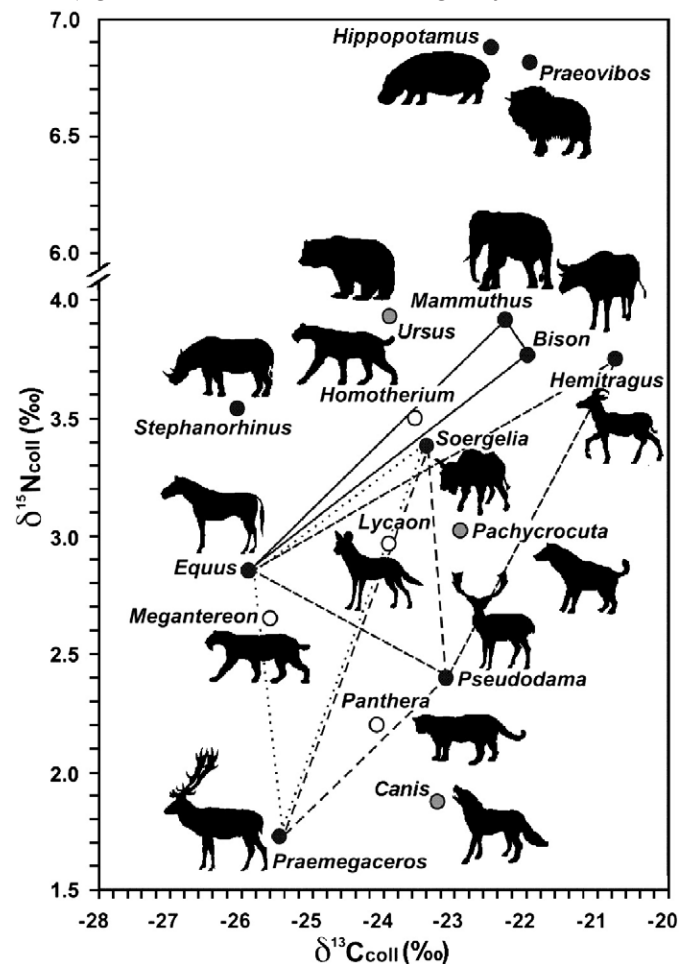


Fig. 6. Plot of $\delta^{13}\text{C}$ and $\delta^{15}\text{N}$ values for carnivore and ungulate species from Venta Micena, corrected for trophic fractionation ($\Delta\delta^{13}\text{C}=0.8\text{‰}$, $\Delta\delta^{15}\text{N}=2.8\text{‰}$). Each of the four hypercarnivore species lies within the triangle defined by its three most probable prey species. According to the linear mixing model (Phillips, 2001), the contribution to carnivore diet of each prey defining a vertex in the triangle is obtained as the distance from this vertex to the opposed side in relation to its distance to the predator (both measured on the line connecting prey and predator). Black circles: ungulates; white circles: hypercarnivores; gray circles: omnivores and bone-cracking hyena.

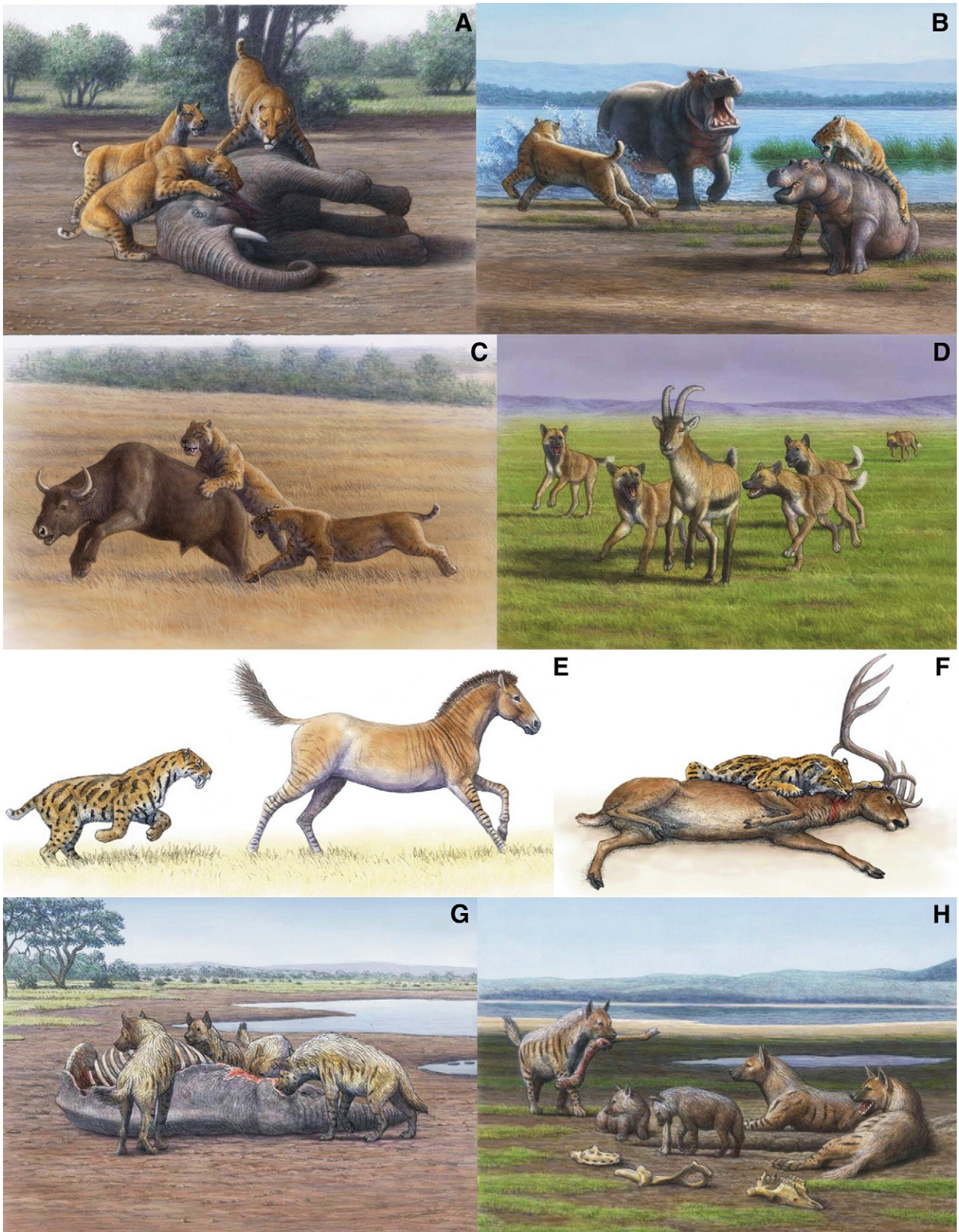


Fig. 7. Reconstruction of the predatory behaviour of the early Pleistocene hypercarnivores preserved in Venta Micena, according to biogeochemical and ecomorphological inferences. Machairodont *Homotherium latidens*, a pursuit predator, hunted subadult elephants (A) and juveniles of other megaherbivore species such as hippo (B), but these prey represented a minor fraction of its diet, which predominantly included ungulates of medium-to-large size from open environment such as bison (C) and horse. Sabre-tooth *Megantereon whitei*, an ambusher, hunted ungulates from open habitat such as horse (D) and browsing deer from forest (E). The hypercarnivorous canid *Lycaon lycaonoides* probably had a pack-hunting behaviour similar to that of modern African painted dogs, with small-to-medium sized ungulates such as goat as their main prey (F). The giant hyena, *Pachycrocuta brevirostris*, scavenged ungulate carcasses left by the hypercarnivores (G) and transported skeletal elements to the denning site (H), a conclusion also supported by taphonomic evidence (Palmqvist et al., 1996; Arribas and Palmqvist, 1998; Palmqvist and Arribas, 2001). Drawings by Mauricio Antón.

megafauna or that the large sabre-tooth *H. latidens* pursued small ungulates; see discussion in Palmqvist et al., 1996), which would in turn distort the estimates obtained for the more probable prey.

The $\delta^{13}\text{C}$ – $\delta^{15}\text{N}$ plot displayed on Fig. 6 shows the prey combinations for the four hypercarnivores under the most realistic scenario according to previous ecomorphological studies on the Venta Micena predators and their analogies to modern carnivores (Palmqvist et al., 1996, 2003; Palmqvist and Arribas, 2001). It is worth introducing, however, a cautionary note on the reliability of the contributions of each prey to the diet of each predator, as they would vary if other enrichment factors are used. According to our results (Fig. 6), the preferred preys of *H. latidens* were grazing and mixed-feeding herbivores from open habitat of medium-to-large size, *Bison* sp. (52%), *E. altidens* (38%) and *M. meridionalis* (10%) (Fig. 7 A, C). The likelihood of such specialized hunting behaviour is evident in the case of the related North American species *H. serum*, known in high numbers from the late Pleistocene site of Friesenhahn cave, a locality interpreted as a sabre-tooth's den and associated with numerous skeletal remains of adult bison and juvenile mammoths (Marean and Ehrhardt, 1995). The diet of sabre-tooth *M. whitei* includes *E. altidens* (59%), *P. verticornis* (31%) and *S. minor* (10%) (Fig. 7 E, F). The jaguar *P. gombaszoegensis* preyed upon *P. verticornis* (43%), *Pseudodama* sp. (38%) and *S. minor* (19%). Finally, the pack hunting *L. lycaonoides* was likely the most versatile predator of this early Pleistocene community due to its social behaviour (Palmqvist et al., 1999) and had a diet that included *E. altidens* (58%), *H. albus* (30%) and *Pseudodama* sp. (12%), which are low-to-medium sized ungulates from open habitat (Fig. 7 D). This combination of prey species is not unreasonable for *L. lycaonoides*, as modern painted dogs show similar predatory habits in the Serengeti, where Thomson's gazelle and zebra represent 38% and 20% of prey captures, respectively (Malcolm and Van Lawick, 1975).

The distribution of ungulate prey described above, based on isotopic signatures, reflect resource partitioning among sympatric predators in Venta Micena. According with the results obtained, coursing carnivores *H. latidens* and *L. lycaonoides* hunted ungulate prey in open habitat, while *M. whitei* and *P. gombaszoegensis* ambushed their prey in the margins between forest and savannah. This is congruent with the palaeoenvironmental reconstruction of Venta Micena, which is interpreted as a wooded savannah (Mendoza et al., 2005). It is interesting to note that the short-faced hyena, *P. brevirostris*, a species specializing in scavenging the prey of hypercarnivores, shows a $\delta^{15}\text{N}$ value (Fig. 3) that matches the one expected for a carnivore that consumed all of the ungulates from open habitat preserved in the faunal assemblage (Fig. 7 G, H).

Fig. 8 shows the average frequencies of ungulate species estimated for a hypothetical death assemblage based on the expectations of the

dual linear mixing model. Such frequencies were calculated assuming that: 1) each carnivore exploited the carcasses of its prey to the same degree; and 2) that each predator contributed similar proportions of kills to the death assemblage collected by the hyenas. This theoretical assemblage was compared with the relative frequencies of herbivores in Venta Micena, based on NISP counts after correction for preservational bias related to body size (Arribas and Palmqvist, 1998). In general terms, there are only relatively minor differences between the expected and observed abundance for most ungulate species. This suggests that the hyenas scavenged the ungulate carcasses in the proportions in which they were available and confirms the accuracy of the estimates obtained with the mixing model on the diet of the Venta Micena predators.

6. Conclusions

Patterns of abundance of stable-isotopes of bone collagen ($\delta^{13}\text{C}$, $\delta^{15}\text{N}$) and bioapatite ($\delta^{18}\text{O}$) are a useful proxy for reconstructing the trophic structure of the early Pleistocene large mammal community preserved at Venta Micena, and help also in deciphering the relationships between predators and their potential prey. Carbon-isotope ratios reveal physiologic differences between hindgut and foregut fermenting ungulates related to their digestive systems and the differential assimilation of cellulose, with perissodactyls showing a lower isotopic enrichment than elephants and artiodactyls from open habitat. The low values seen in cervids suggest that they were mixed feeders or browsers in closed habitat. Nitrogen-isotope ratios of carnivore and herbivore species reflect the isotopic enrichment expected from increasing one trophic level, indicating that the collagen preserved was not diagenetically altered. All ungulate species except the hippo and the muskoxen record isotopic values that agree with a diet of N_2 -fixing plants. Cervids show depleted $\delta^{15}\text{N}$ values resulting from soil acidity in forest, which confirm a browsing diet in closed habitat. The high nitrogen ratio of *H. antiquus* suggests that this species fed predominantly on aquatic vegetation. In the case of *Praeovibos* sp., this mountainous species probably fed on lichens. Oxygen-isotopes of enamel and bone apatite reveal that fallow deer *Pseudodama* and bovids *Hemitragus* and *Soergelia* derived most of their water requirements from the vegetation rather than from drinking. The low $\delta^{18}\text{O}$ values of megacrine deer *Praemegaceros* and of megaherbivores *Stephanorhinus*, *Hippopotamus* and *Mammuthus* suggest a greater degree of water dependence for these species.

Carbon- and nitrogen-isotope ratios in carnivores reflect resource partitioning among sympatric predators, providing interesting clues on predator–prey relationships within this ancient community. The application of the dual linear mixing model allows estimating quantitatively the contribution of several ungulate preys to the diet

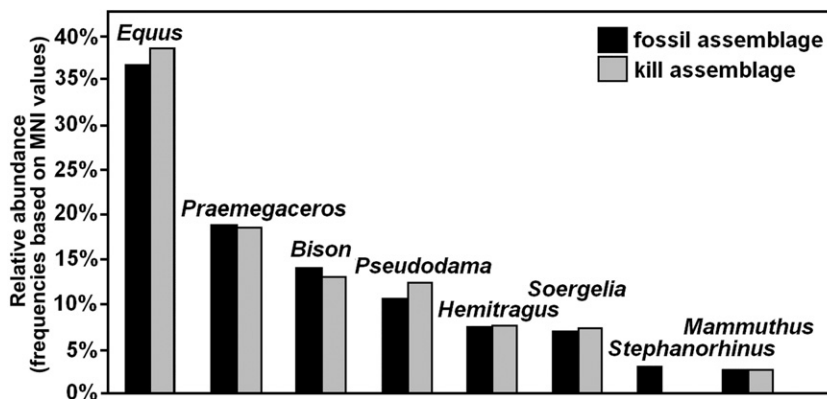


Fig. 8. Comparison between the relative abundance of ungulates in the large mammals assemblage from Venta Micena, corrected for taphonomic bias resulting from differences in body mass (Arribas and Palmqvist, 1998), and the relative frequencies in which these species were hunted by the four hypercarnivores, deduced in this article from the application of the linear mixing model and assuming that each predator contributed similarly to the kill assemblage collected by the hyenas.

of each hypercarnivore. Specifically, the scimitar-cat *Homotherium*, a coursing predator, focused on herbivores from open habitat of relatively large size. The diet of *Megantereon* and the European jaguar, *P. gombaszogensis*, included browsing herbivores from closed habitat such as deer, although horses seem to have been the main prey of the ambushing sabre-tooth. The pack-hunting canid *Lycaon* consumed grazing ungulates from open habitat such as goat and horse. Finally, carbon- and nitrogen-isotopes of the short-faced hyena *Pachycrocuta* match the values expected for a carnivore that scavenged all of the ungulates preserved in the faunal assemblage, especially those that lived in open environments.

Acknowledgments

K. Fox-Dobbs, M.J. Kohn, B. Martínez-Navarro, J. McDonald, C. Nedin, C. Trueman, S.L. Wing and an anonymous reviewer provided insightful comments on an earlier version of the manuscript. Funding and analytical facilities for biogeochemical analyses were provided by the University of Málaga, Royal Holloway University of London and at the Stable-Isotope Biogeochemistry Laboratory at McMaster University.

References

- Ambrose, S.H., DeNiro, M.J., 1986. The isotopic ecology of East African mammals. *Oecologia* 69, 395–406.
- Anadón, P., Julià, R., 1990. Hydrochemistry from Sr and Mg contents of ostracodes in Pleistocene lacustrine deposits, Baza Basin (SE Spain). *Hydrobiologia* 197, 291–303.
- Anadón, P., Utrilla, R., Julià, R., 1994. Palaeoenvironmental reconstruction of a Pleistocene lacustrine sequence from faunal assemblages and ostracode shell geochemistry, Baza Basin, SE Spain. *Palaeogeography, Palaeoclimatology, Palaeoecology* 111, 191–205.
- Andrews, P., Lord, J., Nesbit-Evans, E.M., 1979. Patterns of ecological diversity in fossil and modern mammalian faunas. *Biological Journal of the Linnean Society* 11, 177–205.
- Anyonge, W., 1996. Locomotor behaviour in Plio-Pleistocene sabre-tooth cats: a biomechanical analysis. *Journal of Zoology* 238, 395–413.
- Arribas, A., Palmqvist, P., 1998. Taphonomy and palaeoecology of an assemblage of large mammals: hyaenid activity in the lower Pleistocene site at Venta Micena (Orce, Guadix-Baza Basin, Granada, Spain). *Geobios* 31 (suppl.), 3–47.
- Arribas, A., Palmqvist, P., 1999. On the ecological connection between sabre-tooths and hominids: faunal dispersal events in the lower Pleistocene and a review of the evidence for the first human arrival in Europe. *Journal of Archaeological Science* 26, 571–585.
- Ayliffe, L.K., Lister, A.M., Chivas, A.R., 1992. The preservation of glacial-interglacial climatic signatures in the oxygen isotopes of elephant skeletal phosphate. *Palaeogeography, Palaeoclimatology, Palaeoecology* 99, 179–191.
- Barboza, P.S., Reynolds, P.R., 2004. Monitoring nutrition of a large grazer: muskoxen on the Arctic Refuge. *International Congress Series* 1275, 327–333.
- Bell, R.H.V., 1971. A grazing ecosystem in the Serengeti. *Scientific American* 225, 86–93.
- Biknevicius, A.R., Van Valkenburgh, B., 1996. Design for killing: craniodental adaptations of predators. In: Gittleman, J.L. (Ed.), *Carnivore Behavior, Ecology, and Evolution*, vol. 2. Cornell University Press, Ithaca, NY, pp. 393–428.
- Bocherens, H., Drucker, D., 2003. Trophic level isotopic enrichment of carbon and nitrogen in bone collagen: case studies from recent and ancient terrestrial ecosystems. *International Journal of Osteoarchaeology* 13, 46–53.
- Bocherens, H., Billiou, D., Patou-Mathis, M., Otte, M., Bonjean, D., Toussaint, M., Mariotti, A., 1999. Palaeoenvironmental and palaeodietary implications of isotopic biogeochemistry of late interglacial Neanderthal and mammal bones in Scladina Cave (Belgium). *Journal of Archaeological Science* 26, 599–607.
- Bocherens, H., Billiou, D., Mariotti, A., Toussaint, M., Patou-Mathis, M., Bonjean, D., Otte, M., 2001. New isotopic evidence for dietary habits of Neanderthals from Belgium. *Journal of Human Evolution* 40, 497–505.
- Bocherens, H., Fogel, M.L., Tuross, N., Zeder, M., 1995. Trophic structure and climatic information from isotopic signatures in Pleistocene cave fauna of Southern England. *Journal of Archaeological Science* 22, 327–340.
- Bocherens, H., Koch, P.L., Mariotti, A., Geraads, D., Jaeger, J.J., 1996a. Isotopic biogeochemistry (^{13}C , ^{18}O) and mammalian enamel from African Pleistocene hominid sites. *Palaio* 11, 306–318.
- Bocherens, H., Pacaud, G., Petr, A., Lazarev, P.A., Mariotti, A., 1996b. Stable isotope abundances (^{13}C , ^{15}N) in collagen and soft tissues from Pleistocene mammals from Yakutia: implications for the palaeobiology of the mammoth steppe. *Palaeogeography, Palaeoclimatology, Palaeoecology* 126, 31–44.
- Bocherens, H., Drucker, D.G., Billiou, D., Patou-Mathis, M., Vandermeersch, B., 2005. Isotopic evidence for diet and subsistence pattern of the Saint-Césaire I Neanderthal: review and use of a multi-source mixing model. *Journal of Human Evolution* 49, 71–87.
- Boisserie, J.R., Zazzo, A., Merceron, G., Blondel, C., Vignaud, P., Likius, A., Taïso-Mackaye, H., Brunet, M., 2005. Diets of modern and late Miocene hippopotamids: evidence from carbon isotope composition and micro-wear of tooth enamel. *Palaeogeography, Palaeoclimatology, Palaeoecology* 221, 153–174.
- Bryant, J.D., Froelich, P.N., 1995. A model of oxygen isotope fractionation in body water of large mammals. *Geochimica et Cosmochimica Acta* 59, 4523–4537.
- Bryant, J.D., Koch, P.L., Froelich, P.N., Showers, W.J., Genna, B.J., 1996. Oxygen isotope partitioning between phosphate and carbonate in mammalian apatite. *Geochimica et Cosmochimica Acta* 60, 5145–5148.
- Cerling, T.E., Harris, J.M., 1999. Carbon isotope fractionation between diet and bioapatite in ungulate mammals and implications for ecological and paleoecological studies. *Oecologia* 120, 347–363.
- Cerling, T.E., Harris, J.M., Leakey, M.G., 1999. Browsing and grazing in elephants: the isotope record of modern and fossil proboscideans. *Oecologia* 120, 364–374.
- Cerling, T.E., Harris, J.M., Passey, B.H., 2003. Diets of east African bovidae based on stable isotope analysis. *Journal of Mammalogy* 84, 456–470.
- Chivas, A.R., De Deckker, P., Shelley, J.M.G., 1985. Strontium content of ostracods indicates lacustrine palaeosalinity. *Nature* 316, 251–253.
- Chivas, A.R., De Deckker, P., Shelley, J.M.G., 1986. Magnesium content of non-marine ostracod shells: a new palaeosalinometer and palaeothermometer. *Palaeogeography, Palaeoclimatology, Palaeoecology* 54, 43–61.
- Clauss, M., Frey, R., Kiefer, B., Lechner-Doll, M., Loehein, W., Polster, C., Rössner, G.E., Streich, W.J., 2003. The maximum attainable body size of herbivorous mammals: morphophysiological constraints on foregut, and adaptations of hindgut fermenters. *Oecologia* 136, 14–27.
- Coltrain, J.B., Harris, J.M., Cerling, T.E., Ehleringer, J.R., Dearing, M.-D., Ward, J., Allen, J., 2004. Rancho La Brea stable isotope biogeochemistry and its implications for the palaeoecology of late Pleistocene, coastal southern California. *Palaeogeography, Palaeoclimatology, Palaeoecology* 205, 199–219.
- Crutzen, P.J., Asleman, I., Seiler, W., 1986. Methane production by domestic animals, wild ruminants, and other herbivorous fauna, and humans. *Tellus* 38B, 271–284.
- Damuth, J., 1992. Taxon-free characterization of animal communities. In: Behrensmeier, A.K., Damuth, J.D., DiMichelle, W.A., Potts, R., Sues, H.D., Wing, S.L. (Eds.), *Terrestrial Ecosystems through Time: Evolutionary Paleocology of Terrestrial Plants and Animals*. The University of Chicago Press, Chicago, pp. 183–203.
- DeNiro, M.J., Epstein, S., 1978. Influence of diet on the distribution of carbon isotopes in animals. *Geochimica et Cosmochimica Acta* 42, 495–506.
- Demment, M.W., Van Soest, P.J., 1985. A nutritional explanation for body-size patterns of ruminant and nonruminant herbivores. *American Naturalist* 125, 641–672.
- Drucker, D., Bocherens, H., 2004. Carbon and nitrogen stable isotopes as tracers of change in diet breadth during Middle and Upper Palaeolithic in Europe. *International Journal of Osteoarchaeology* 14, 162–177.
- Drucker, D., Bocherens, H., Bridault, A., Billiou, D., 2003. Carbon and nitrogen isotopic composition of red deer (*Cervus elaphus*) collagen as a tool for tracking palaeoenvironmental change during the Late-Glacial and Early Holocene in the northern Jura (France). *Palaeogeography, Palaeoclimatology, Palaeoecology* 195, 375–388.
- Duncan, P., Foote, T.J., Gordon, I.J., Gakahu, C.G., Loyd, M., 1990. Comparative nutrient extraction from forages by grazing bovines and equids: a test of the nutritional model of equid-ovine competition and coexistence. *Oecologia* 84, 411–418.
- Edwards, G., Walker, D.A., 1983. C_3 , C_4 : Mechanisms, and Cellular and Environmental Regulation, of Photosynthesis. Blackwell Scientific Publications, Oxford.
- Fernández-Mosquera, D., Vila-Taboada, M., Grandal-d'Anglade, A., 2001. Stable isotopes ($\delta^{13}\text{C}$, $\delta^{15}\text{N}$) from the cave bear (*Ursus spelaeus*): a new approach to its palaeoenvironment and dormancy. *Proceedings of the Royal Society of London B*, vol. 268, pp. 1159–1164.
- Flecker, R., de Villiers, S., Ellam, R.M., 2002. Modelling the effect of evaporation on the salinity- $^{87}\text{Sr}/^{86}\text{Sr}$ relationship in modern and ancient marginal-marine systems: the Mediterranean Messinian Salinity Crisis. *Earth and Planetary Science Letters* 203, 221–233.
- Fizet, M., Mariotti, A., Bocherens, H., Lange-Badré, B., Vandermeersch, B., Borel, J.P., Bellon, G., 1995. Effect of diet, physiology and climate on carbon and nitrogen isotopes of collagen in a late Pleistocene anthropic paleoecosystem (France, Charente, Marillac). *Journal of Archaeological Science* 22, 67–79.
- Fortelius, M., Kappelman, J., 1993. The largest land mammal ever imagined. *Zoological Journal of the Linnean Society* 107, 85–101.
- Fortelius, M., Solounias, N., 2000. Functional characterization of ungulate molars using the abrasion-attrition wear gradient: a new method for reconstructing palaeodiets. *American Museum Novitates*, 3301, 1–36.
- Geist, V., 1974. On the relationship of social evolution and ecology in ungulates. *American Zoologist* 14, 205–220.
- Gröcke, D.R., 1997a. Stable-isotope studies on the collagen and hydroxylapatite components of fossils: palaeoecological implications. *Lethaia* 30, 65–78.
- Gröcke, D.R., 1997b. Distribution of C_3 and C_4 plants in the late Pleistocene of South Australia recorded by isotope biogeochemistry of collagen in megafauna. *Australian Journal of Botany* 45, 607–617.
- Gröcke, D.R., Bocherens, H., 1996. Isotopic investigation of an Australian island environment. *Comptes Rendus de l'Académie des Sciences de Paris, Serie II* 322, 713–719.
- Gröcke, D.R., Bocherens, H., Mariotti, A., 1997. Annual rainfall and nitrogen-isotope correlation in macropod collagen: application as a palaeoprecipitation indicator. *Earth and Planetary Science Letters* 153, 279–285.
- Gröcke, D.R., Palmqvist, P., Arribas, A., 2002. Biogeochemical inferences on the Early Pleistocene large mammal paleocommunity from Venta Micena (Guadix-Baza basin, southeastern Spain). In: De Renzi, M. (Ed.), *Current Topics in Taphonomy and Fossilization*. Ayuntamiento de Valencia, pp. 127–142.
- Harris, J.M., Cerling, T.E., 2002. Dietary adaptations of extant and Neogene African suids. *Journal of Zoology* 256, 45–54.
- Hedges, R.E.M., 2003. On bone collagen-apatite-carbonate isotopic relationships. *International Journal of Osteoarchaeology* 13, 66–79.

- Hoppe, K.A., 2004. Late Pleistocene mammoth herd structure, migration patterns, and Clovis hunting strategies inferred from isotopic analyses of multiple death assemblages. *Paleobiology* 30, 129–145.
- Hoppe, K.A., Koch, P.L., Carlson, R.W., Webb, S.D., 1999. Tracking mammoths and mastodons: reconstruction of migratory behavior using strontium isotope ratios. *Geology* 27, 439–442.
- Hu, F.S., Ito, E., Brubaker, L.B., Anderson, P.M., 1998. Ostracode geochemical record of Holocene climatic change and implications for vegetational response in the Northwestern Alaska range. *Quaternary Research* 49, 86–95.
- Illius, A.W., Gordon, I.J., 1992. Modelling the nutritional ecology of ungulate herbivores: evolution of body size and competitive interactions. *Oecologia* 89, 428–434.
- Janis, C.M., 1976. The evolutionary strategy of the Equidae and the origins of rumen and caecal fermentation. *Evolution* 30, 757–774.
- Janis, C.M., Ehrhardt, D., 1988. Correlation of the relative muzzle width and relative incisor width with dietary preferences in ungulates. *Zoological Journal of the Linnean Society* 92, 267–284.
- Janis, C.M., Gordon, I.J., Illius, A.W., 1984. Modelling equid/ruminant competition in the fossil record. *Historical Biology* 8, 15–29.
- Jarman, P.J., 1974. The social organization of antelope in relation to their ecology. *Behaviour* 48, 215–267.
- Jenkins, S.G., Partridge, S.T., Stephenson, T.R., Farley, S.D., Robbins, C.T., 2001. Nitrogen and carbon isotope fractionation between mothers, neonates, and nursing offspring. *Oecologia* 129, 336–341.
- Jones, A.M., O'Connell, T.C., Young, E.D., Scott, K., Buckingham, C.M., Iacumin, P., Brasier, M.D., 2001. Biogeochemical data from well preserved 200 ka collagen and skeletal remains. *Earth and Planetary Science Letters* 193, 143–149.
- Justice, K.E., Smith, F.A., 1992. A model of dietary fiber utilization by small mammalian herbivores, with empirical results for *Neotoma*. *The American Naturalist* 139, 398–416.
- Kleiber, M., 1975. *The Fire of Life: An Introduction to Animal Energetics*. Krieger Publishing Company, NY.
- Klein, D.R., Bay, C., 1994. Resource partitioning by mammalian herbivores in the high Arctic. *Oecologia* 97, 439–450.
- Koch, P.L., 1998. Isotopic reconstruction of past continental environments. *Annual Review of Earth and Planetary Sciences* 26, 573–613.
- Koch, P.L., Fisher, D.C., Dettman, D., 1989. Oxygen isotope variations in the tusks of extinct proboscideans: a measure of season of death and seasonality. *Geology* 17, 515–519.
- Koch, P.L., Heisinger, J., Moss, C., Carlson, R.W., Fogel, M.L., Behrensmeyer, A.K., 1995. Isotopic tracking of the diet and home range of African elephants. *Science* 267, 1340–1343.
- Koch, P.L., Hoppe, K.A., Webb, S.D., 1998. The isotopic ecology of late Pleistocene mammals in North America. Part 1. Florida. *Chemical Geology* 152, 119–138.
- Kohn, M.J., 1996. Predicting animal $\delta^{18}\text{O}$: accounting for diet and physiological adaptation. *Geochimica et Cosmochimica Acta* 60, 4811–4829.
- Kohn, M.J., Schoeninger, M.J., Valley, J.W., 1996. Herbivore tooth oxygen isotope compositions: effects of diet and physiology. *Geochimica et Cosmochimica Acta* 60, 3889–3896.
- Lee-Thorp, J., Van der Merwe, N.J., 1987. Carbon isotope analysis of fossil bone apatite. *South African Journal of Science* 83, 712–715.
- Lewis, M.E., 1997. Carnivorous paleoguilds of Africa: implications for hominid food procurement strategies. *Journal of Human Evolution* 32, 257–288.
- Loehlein, W., Kienzle, E., Wiesner, H., Clauss, M., 2003. Investigations on the use of chromium oxide as an inert external marker in captive Asian elephants (*Elephas maximus*): passage and recovery rates. In: Fidgett, A., Clauss, M., Ganslosser, U., Hatt, J.M., Nijboer, J. (Eds.), *Zoo animal nutrition*, vol. II. Filander, Fürth, Germany, pp. 223–232.
- MacFadden, B.J., 2000. Cainozoic mammalian herbivores from the Americas: reconstructing ancient diets and terrestrial communities. *Annual Review of Ecology and Systematics* 31, 33–59.
- Malcolm, J.R., Van Lawick, H., 1975. Notes on wild dogs (*Lycan pictus*) hunting zebras. *Mammalia* 39, 231–240.
- Marean, C.W., Ehrhardt, C.L., 1995. Paleoanthropological and paleoecological implications of the taphonomy of a sabretooth's den. *Journal of Human Evolution* 29, 515–547.
- McNab, B.K., 1986. The influence of food habits on the energetics of eutherian mammals. *Ecological Monographs* 56, 1–19.
- McNaughton, S.J., Georgiadis, N.J., 1986. Ecology of African grazing and browsing mammals. *Annual Review of Ecology and Systematics* 17, 39–65.
- McNulty, T., Calkins, A., Ostrom, P., Gandhi, H., Gottfried, M., Martin, L., Gage, D., 2002. Stable isotope values of bone organic matter: artificial diagenesis experiments and paleoecology of Natural Trap Cave, Wyoming. *Palaio* 17, 36–49.
- Mendoza, M., Palmqvist, P., 2008. Hypsodonty in ungulates: an adaptation for grass consumption or for foraging in open habitat? *Journal of Zoology* 274, 134–142.
- Mendoza, M., Janis, C.M., Palmqvist, P., 2002. Characterizing complex craniodental patterns related to feeding behaviour in ungulates: a multivariate approach. *Journal of Zoology* 258, 223–246.
- Mendoza, M., Janis, C.M., Palmqvist, P., 2005. Ecological patterns in the trophic-size structure of large mammal communities: a 'taxon-free' characterization. *Evolutionary Ecology Research* 7, 505–530.
- Metges, C., Kempe, K., Schmidt, H.L., 1990. Dependence of the carbon isotope contents of breath carbon dioxide, milk, serum and rumen fermentation products on the value of food in dairy cows. *Brown Journal of Nutrition* 63, 187–196.
- Miller, E.K., Blum, J.D., Friedland, A.J., 1993. Determination of soil exchangeable-cation loss and weathering rates using Sr isotopes. *Nature* 362, 438–441.
- Novak, R.M., 1999. *Walker's Mammals of the World*. The Johns Hopkins University Press, Baltimore and London.
- Ortiz, J.E., Torres, T., Delgado, A., Reyes, E., Llamas, J.F., Soler, V., Raya, J., 2006. Pleistocene paleoenvironmental evolution at continental middle latitude inferred from carbon and oxygen stable isotope analysis of ostracodes from the Guadix-Baza Basin (Granada, SE Spain). *Palaeogeography, Palaeoclimatology, Palaeoecology* 240, 536–561.
- Ostrom, P.H., Macko, S.A., Engel, M.H., Russell, D.A., 1993. Assessment of trophic structure of Cretaceous communities based on stable nitrogen isotope analysis. *Geology* 21, 491–494.
- Palmqvist, P., Arribas, A., 2001. Taphonomic decoding of the paleobiological information locked in a lower Pleistocene assemblage of large mammals. *Paleobiology* 27, 512–530.
- Palmqvist, P., Martínez-Navarro, B., Arribas, A., 1996. Prey selection by terrestrial carnivores in a lower Pleistocene paleocommunity. *Paleobiology* 22, 514–534.
- Palmqvist, P., Arribas, A., Martínez-Navarro, B., 1999. Ecomorphological analysis of large canids from the lower Pleistocene of southeastern Spain. *Lethaia* 32, 75–88.
- Palmqvist, P., Mendoza, M., Arribas, A., Gröcke, D.R., 2002. Estimating the body mass of Pleistocene canids: discussion of some methodological problems and a new 'taxon free' approach. *Lethaia* 35, 358–360.
- Palmqvist, P., Gröcke, D.R., Arribas, A., Fariña, R., 2003. Paleocological reconstruction of a lower Pleistocene large mammals community using biogeochemical ($\delta^{13}\text{C}$, $\delta^{15}\text{N}$, $\delta^{18}\text{O}$, Sr:Zn) and ecomorphological approaches. *Paleobiology* 29, 204–228.
- Parker, K.L., Barboza, P.S., Stephenson, T.R., 2005. Protein conservation in female caribou (*Rangifer tarandus*): effects of decreasing diet quality during winter. *Journal of Mammalogy* 86, 610–622.
- Parra, R., 1978. Comparison of foregut and hindgut fermentation in herbivores. In: Montgomery, G.G. (Ed.), *The Ecology of Arboreal Folivores*. Smithsonian Institution Press, Washington, pp. 205–230.
- Pérez-Barbería, F.J., Gordon, I.J., 2001. Relationships between oral morphology and feeding style in the Ungulata: a phylogenetically controlled evaluation. *Proceedings of the Royal Society of London* 268, 1021–1030.
- Phillips, D.L., 2001. Mixing models in analyses of diet using multiple stable isotopes: a critique. *Oecologia* 127, 166–170.
- Phillips, D.L., Gregg, J.W., 2001. Uncertainty in source partitioning using stable isotopes. *Oecologia* 127, 171–179.
- Phillips, D.L., Gregg, J.W., 2003. Source partitioning using stable isotopes: coping with too many sources. *Oecologia* 136, 261–269.
- Phillips, D.L., Koch, P.L., 2002. Incorporating concentration dependence in stable isotope mixing models. *Oecologia* 130, 114–125.
- Phillips, D.L., Newsome, S.D., Gregg, J.W., 2005. Combining sources in stable isotope mixing models: alternative methods. *Oecologia* 144, 520–527.
- Price, T.D., Connor, M., Parsen, J.D., 1985. Bone chemistry and the reconstruction of diet: strontium discrimination in white-tailed deer. *Journal of Archaeological Science* 12, 419–442.
- Prins, R.A., Kreulen, D.A., 1991. Comparative aspects of plant cell wall digestion in mammals. In: Hoshino, S., Onodera, R., Minoto, H., Itabashi, H. (Eds.), *The Rumen Ecosystem: the Microbial Metabolism and its Regulation*. Japan Scientific Society Press, Tokyo, pp. 109–121.
- Reed, K.E., 1998. Using large mammal communities to examine ecological and taxonomic structure and predict vegetation in extant and extinct assemblages. *Paleobiology* 24, 384–408.
- Richards, M.P., Hedges, R.E.M., 2003. Variations in bone collagen $\delta^{13}\text{C}$ and $\delta^{15}\text{N}$ values of fauna from Northwest Europe over the last 40,000 years. *Palaeogeography, Palaeoclimatology, Palaeoecology* 193, 261–267.
- Richards, M.P., Pettitt, P.B., Trinkaus, E., Smith, F.H., Paunovic, M., Karavanic, I., 2000. Neanderthal diet at Vindija and Neanderthal predation: the evidence from stable isotopes. *Proceedings of the National Academy of Sciences USA* 97, 7663–7666.
- Robinson, D., 2001. $\delta^{15}\text{N}$ as an integrator of the nitrogen cycle. *Trends in Ecology and Evolution* 16, 153–162.
- Rodière, E., Bocherens, H., Angibault, J.M., Mariotti, A., 1996. Particularités isotopiques de l'azote chez le chevreuil (*Capreolus capreolus* L.): implications pour les reconstitutions paléoenvironnementales. *Comptes Rendus de l'Académie des Sciences de Paris, Serie II* 323, 179–185.
- Schwarz, H.P., 1991. Some theoretical aspects of isotope paleodiet studies. *Journal of Archaeological Science* 18, 261–275.
- Schwarz, H.P., Tossa Dupras, L., Fairgrieve, S.I., 1999. ^{15}N enrichment in the Sahara: in search of a global relationship. *Journal of Archaeological Science* 26, 629–636.
- Schwarm, A., Ortmann, S., Hofer, H., Streich, W.J., Flach, E.J., Kühne, R., Hummel, J., Castell, J.C., Clauss, M., 2006. Digestion studies in captive Hippopotamidae: a group of large ungulates with an unusually low metabolic rate. *Journal of Animal Physiology and Animal Nutrition* 90, 300–308.
- Schulze, E., Lohmeyer, S., Giese, W., 1998. Determination of C-13/C-12-ratios in rumen produced methane and CO₂ of cows, sheep and camels. *Isotopes in Environmental and Health Studies* 34, 75–79.
- Sealy, J.C., Van der Merwe, N.J., Lee-Thorp, J.A., Lanham, J.L., 1987. Nitrogen isotopic ecology in southern Africa: implications for environmental and dietary tracing. *Geochimica et Cosmochimica Acta* 51, 2707–2717.
- Shipley, L.A., Gross, J.E., Spalinger, D.E., Thompson-Hobbs, N., Wunder, B.A., 1994. The scaling of intake rate in mammalian herbivores. *The American Naturalist* 143, 1055–1082.
- Sillen, A., Lee-Thorp, J.A., 1994. Trace element and isotopic aspects of predator-prey relationships in terrestrial foodwebs. *Palaeogeography, Palaeoclimatology, Palaeoecology* 107, 243–255.
- Smith, B.N., Epstein, S., 1971. Two categories of $^{13}\text{C}/^{12}\text{C}$ ratios for higher plants. *Plant Physiology* 47, 380–384.
- Soligo, C., Andrews, P., 2005. Taphonomic bias, taxonomic bias and historical non-equivalence of faunal structure in early hominin localities. *Journal of Human Evolution* 49, 206–229.

- Solounias, N., Moelleken, S.M.C., 1993. Tooth microwear and premaxillary shape of an archaic antelope. *Lethaia* 26, 261–268.
- Sponheimer, M., Lee-Thorp, J.A., 2001. The oxygen isotope composition of mammalian enamel carbonate from Morea State, South Africa. *Oecologia* 126, 153–157.
- Springer, M.S., Cleven, G.C., Madsen, O., de Jong, W.W., Waddell, V.G., Amrine, H.M., Stanhope, M.J., 1997. Edemic African mammals shake the phylogenetic tree. *Nature* 388, 61–64.
- Szepanski, M.M., Ben-David, M., Van Ballenberghe, V., 1999. Assessment of salmon resources in the diet of the Alexander Archipelago wolf using stable isotope analysis. *Oecologia* 120, 327–335.
- Torres, J.M., Borja, C., García-Olivares, E., 2002. Immunoglobulin G in 1.6 million-year-old fossil bones from Venta Micena (Granada, Spain). *Journal of Archaeological Science* 29, 167–175.
- Turner, A., Antón, M., 1996. The giant hyaena, *Pachycrocuta brevirostris* (Mammalia, Carnivora, Hyaenidae). *Geobios* 29, 455–468.
- Van der Merwe, N.J., 1989. Natural variation in ^{13}C concentration and its effect on environmental reconstruction using $^{13}\text{C}/^{12}\text{C}$ ratios in animal bones. In: Pride, T.D. (Ed.), *The chemistry of prehistoric human bone*. Cambridge University Press, Cambridge, pp. 105–125.
- Van Soest, P.J., 1994. *Nutritional ecology of the ruminant*, 2nd edn. Cornell University Press, Ithaca. 476 pp.
- Van Soest, P.J., 1996. Allometry and ecology of feeding behavior and digestive capacity in herbivores: a review. *Zoo Biology* 15, 455–479.
- Van Valkenburgh, B., 1985. Locomotor diversity within past and present guilds of large predatory mammals. *Paleobiology* 11, 406–428.
- Van Valkenburgh, B., 1988. Trophic diversity in past and present guilds of large predatory mammals. *Paleobiology* 14, 155–173.
- Vanderklift, M.A., Ponsard, S., 2003. Sources of variation in consumer-diet $\delta^{15}\text{N}$ enrichment: a meta-analysis. *Oecologia* 136, 169–182.
- Vermorel, M., Martin-Rosset, W., Vernet, J., 1997. Energy utilization of twelve forages or mixed diets for maintenance by sport horses. *Science* 275, 157–167.
- Virginia, R.A., Jarrell, W.M., Rundel, P.W., Shearer, G., Kohl, D.H., 1989. The use of variation in the natural abundance of ^{15}N to assess symbiotic nitrogen fixation by woody plants. In: Rundel, P.W., Ehleringer, J.R., Nagy, K.A. (Eds.), *Stable Isotopes in Ecological Research*. Springer-Verlag, New York, pp. 345–394.
- Williams, S.H., Kay, R.F., 2001. A comparative test for adaptive explanations for hypsodonty in ungulates and rodents. *Journal of Mammalian Evolution* 8, 207–229.
- Wing, S.L., Sues, H.D., Potts, R., DiMichelle, W.A., Behrensmeier, A.K., 1992. Evolutionary paleoecology. In: Behrensmeier, A.K., Damuth, J.D., DiMichelle, W.A., Potts, R., Sues, H.D., Wing, S.L. (Eds.), *Terrestrial Ecosystems through Time: Evolutionary Paleocology of Terrestrial Plants and Animals*. The University of Chicago Press, Chicago, pp. 1–13.